For Reference

NOT TO BE TAKEN FROM THIS ROOM

For Reference

NOT TO BE TAKEN FROM THIS ROOM

Ex libris
universitatis
albertaensis

UNIVERSITY OF ALBERTA
QUAECUMQUE VERA

University of Alberta
Printing Department

Digitized by the Internet Archive
in 2019 with funding from
University of Alberta Libraries

https://archive.org/details/Narayana1966

1966 (F)
21 D

THE UNIVERSITY OF ALBERTA

SOUND ABSORPTION MEASUREMENTS IN GASES

BY

HELENE NARAYANA

A THESIS
SUBMITTED TO THE FACULTY OF GRADUATE STUDIES IN
PARTIAL FULFILMENT OF THE REQUIREMENTS FOR THE
DEGREE OF DOCTOR OF PHILOSOPHY

DEPARTMENT OF PHYSICS
EDMONTON, ALBERTA
JULY, 1966

UNIVERSITY OF ALBERTA

FACULTY OF GRADUATE STUDIES

The undersigned certify that they have read, and recommend to the Faculty of Graduate Studies for acceptance, a thesis entitled "SOUND ABSORPTION MEASUREMENTS IN GASES", submitted by Hélène Narayana in partial fulfilment of the requirements for the degree of Doctor of Philosophy.

ABSTRACT

Apparatus was built for the purpose of measuring the absorption of sound by the pulse technique in gases at low temperatures. The fixed frequency of operation was 3 Mc/sec, and by varying the pressure of gas, absorption measurements were made at a frequency-to-pressure ratio ranging from 3 to 45 Mc/sec-atm. No reports appear in the literature about the use of the pulse technique at low temperatures.

The instrument was tested for proper operation by measuring the absorption of sound in helium both at room temperature and at liquid nitrogen temperature.

The absorption of ultrasonic waves was measured, at liquid nitrogen temperature, in normal hydrogen and in a para-enriched mixture of hydrogen.

The theory of sound absorption in fluids is summarized: the first part of the treatment deals with the classical absorption due to viscosity and thermal conductivity, while the second part deals with relaxational absorption due to a slowness of energy exchange between the translational and the internal degrees of freedom of a gas molecule. The review of the theory given here is more general than is customarily given on work in gases.

The results are discussed and compared with similar results obtained by different techniques at different

temperatures.

The relaxation time for the $0 \longrightarrow 2$ transition in hydrogen at 76.7 $^{\circ}$K is found to be approximately 2.1×10^{-8} sec. Measurements both in normal hydrogen and in para-enriched hydrogen yield the same value of the relaxation time; this is in contrast to the results of Sluijter, Knaap and Beenakker. The theories for calculation of relaxation times are not precise enough to shed light on this discrepancy.

ACKNOWLEDGEMENTS

The author wishes to thank Prof. S. B. Woods who supervised this project. His constant encouragement and hopeful attitude were most appreciated.

It is also a pleasure to thank Prof. A. B. Bhatia, who in the absence of Prof. Woods, read and corrected this thesis.

The author is grateful to all members of the technical staff, and in particular to Mr. Hank Mc Clung, for their invaluable help.

Financial assistance from the University of Alberta, as well as from the National Research Council, is gratefully acknowledged.

And finally, to a patient, sympathetic and understanding husband, simply but wholeheartedly: Thank you.

TABLE OF CONTENTS

Page

CHAPTER I THEORY 1

INTRODUCTION 1

1. Fundamentals of the phenomenological thermodynamics of irreversible processes. 3
2. Classical sound absorption 11
3. Relaxational absorption 21
4. Relaxational absorption in hydrogen 35

CHAPTER II EXPERIMENT 43

1. Experimental methods 43
2. Apparatus 48
   - A. Mechanical part 49
   - B. Mounting of the transducers 51
   - C. Vacuum system 54
   - D. Electronic circuitry 54
3. Procedure 56

CHAPTER III RESULTS AND DISCUSSION 59

1. Sound absorption measurements in helium at room temperature 59
2. Sound absorption measurements in helium at 76.7 °K 59
3. Sound absorption measurements in normal hydrogen at 76.7 °K 65
4. Sound absorption measurements in para-enriched hydrogen ay 76.7 °K 73

Page
CONCLUSION 86
BIBLIOGRAPHY 88

LIST OF FIGURES

		Page
1.	a) $(C_o/C)^2$ vs $\ln\omega$	32
	b) $\mu(C_o/C)^2$ vs $\ln\omega$	32
	c) μ vs $\ln\omega$	32
2.	a) τ_{pT}	37
	b) τ_{pS}	37
	c) τ_{VS}	37
3.	a) Energy level population in para hydrogen	40
	b) Energy level population in ortho hydrogen	41
4.	Cross section of the apparatus	50
5.	Transducers mount	52
6.	Electronic circuitry	55
7.	Typical record	57
8.	Curve of lnA vs x	58
9.	$\bar{\alpha}'/f$ vs f/p for helium at 296 °K	64
10.	$\bar{\alpha}'/f$ vs f/p for helium at 76.7 °K	68
11.	$\bar{\alpha}'/f$ vs f/p for normal hydrogen at 76.7 °K	71
12.	$\bar{\alpha}'/f$ vs f/p for para-enriched hydrogen at 76.7 °K	77

CHAPTER I

THEORY

Introduction

The propagation of sound in fluids has been a subject of interest for well over a century. The first theoretical treatment of importance on the subject, dates back to 1845. It is due to Stokes, who investigated the effects of viscosity on the propagation of sound. Later, in 1868, Kirchhoff showed that heat conduction in fluids gives rise to an absorption of sound which is of the same order of magnitude as that due to viscosity. A few authors, among whom Lord Rayleigh is prominent, have also evaluated the effect of heat radiation on the propagation of sound in fluids; their estimates showed however, that radiation plays little role in gases, except perhaps, at very low pressures and very high temperatures.

Early experimental works consistently yielded results which indicated that the absorption of sound in gases other than monatomic gases, was much in excess of that predicted by the so-called classical theory.

In 1928, Herzfeld and Rice suggested that the excess absorption of sound in fluids might be due to a phenomenon that they termed "thermal relaxation." Much refined in the following years, this theory has gained wide acceptance, and accounts for a great number of experimental results. Sound absorption data in fluids can yield very valuable information about the nature of the interaction between colliding particles, since the energy transfer depends strongly upon the non-spherical part of that interaction.

A recent treatment of the subject by Bauer,[1] based on the principles of the thermodynamics of irreversible processes, is of particular interest in view of its relatively simple, and surely very elegant solution of such complicated problems as multiple relaxation processes in a three-level gas, or in mixtures of two gases with excitable states.

Therefore, a unified treatment, using the methods of the thermodynamics of irreversible processes, as developed by Meixner, will yield the "classical" sound absorption equations, also known as the Stokes-Navier equations, as well as those for the "anomalous" sound absorption, due to relaxation. Meixner proved that, to a first approximation, the contributions to the absorption of sound from the transport phenomena and those from the internal transitions, are additive. The two problems can thus be treated separately.

Before dealing especially with the topic of sound absorption in gases, a summary of the fundamentals of the method used is given.

1. Fundamentals of the Phenomenological Thermodynamics of Irreversible Processes

The usual inequality of ordinary thermodynamics relates the increase in entropy dS of a system, to its absolute temperature T, and to the heat supplied to it, dQ, namely

$$dS \geq \frac{dQ}{T} \quad . \tag{1-1}$$

(1-1) can be made an equality by writing as follows:

$$dS = \frac{dQ}{T} + d_iS = d_eS + d_iS, \tag{1-2}$$

in which case the differential d_eS represents the entropy supplied to the system by its surroundings, and d_iS represents the entropy produced inside the system; d_iS is always positive.

One of the most important objectives of the thermodynamics of irreversible phenomena is to relate d_iS to the various irreversible phenomena which may occur within the system. In order to do so, it is convenient to use the entropy

production per unit time and unit volume - often called the entropy source strength - as a unit of irreversibility:

$$\sigma = \frac{d_i S}{dt} \qquad (1\text{-}3)$$

Combined with (1-2), the equation expressing the first law of thermodynamics,

$$dU = dQ + dW \,, \qquad (1\text{-}4)$$

becomes

$$dW = dU - T\, d\, S + T\, d_i S = d\, W_{rev} + T\, d_i S \qquad (1\text{-}5)$$

where dU is the increase in internal energy of the system, and $(dW - d\, W_{rev})$ is the work expended or the energy dissipated. The general form of the rate of entropy production is

$$\sigma = \sum_i X_i \, J_i \qquad (1\text{-}6)$$

where the J_i's are the "fluxes" denoting the speed with which the irreversible processes occur, and the X_i's are the thermodynamic "forces" which are related to the non-uniformity of the system (the gradient of the temperature for example).

Since, at equilibrium both the fluxes and the forces disappear, the fluxes are surely functions of the forces. For small departures from equilibrium, as a first approximation

$$J_i = \sum_k L_{ik} X_k, \tag{1-7}$$

where

$$L_{ik} = \frac{\partial J_i}{\partial X_k} \quad . \tag{1-8}$$

Therefore

$$\sigma = \sum_{i,k} L_{ik} X_i X_k \quad . \tag{1-9}$$

The coefficients L_{ik} are called the phenomenological coefficients. Since (1-9) is always positive by virtue of the second law of thermodynamics, the matrix $[L_{ik}]$ is positive definite and is symmetric, i.e., $L_{ik} = L_{ki}$.

The standard procedure to find the phenomenological coefficients, i.e., to set up equation (1-8), is summarised as follows:

From the rate of change of the entropy, which is determined by the variations in the properties of the system, the entropy source strength σ can be calculated. From (1-9) it is readily noted that σ is a sum of scalar products of the form

$$\frac{\partial J_i}{\partial X_k} X_i X_k .$$

In order to determine the rate of change of the entropy of a system, the state of the system must be defined in terms of certain state variables. These state variables are of two kinds: 1) external (e.g. pressure, temperature) variables which need no further comment and, 2) "chemical" variables if reactions occur which change the material composition of the system. Here the term "chemical" is being used rather loosely; excitations of internal degrees of freedom constitute, in this sense, chemical reactions. Thus the chemical variables need to be examined more carefully. When chemical reactions occur in a system, they can be described in terms of two sets of thermodynamically conjugate variables, called the progress variables and the affinities.

The progress variables are best understood as follows: Suppose there are r possible reactions in a system containing N substances. The reaction equations are given by

$$\sum_{i=1}^{N} \nu_{i\alpha} [M_i] \rightleftharpoons \sum \nu'_{i\alpha} [M_i] \quad (\alpha = 1, 2, \ldots r) \tag{1-10}$$

where M_i is the mass of substance i, $\nu_{i\alpha}$ and $\nu'_{i\alpha}$ are the left and right stoichiometric coefficients of substance i in the reaction α. When the reaction α proceeds by a differential amount, $d\,n_i^{\alpha}$ the change in the number of moles of substance i is given by

$$\frac{dn_1^\alpha}{\Delta\nu_{1\alpha}} = \frac{dn_2^\alpha}{\Delta\nu_{2\alpha}} = \text{------} = d\xi_\alpha \qquad (1\text{-}11)$$

where $\Delta\nu_{i\alpha} = \nu'_{i\alpha} - \nu_{i\alpha}$. The total change $d\,n_i$ becomes

$$dn_i = \sum_{\alpha=1}^{r} \Delta\nu_{i\alpha}\, d\xi_\alpha \quad . \qquad (1\text{-}12)$$

$d\xi_\alpha$ represents the differential amount by which reaction α has advanced. The parameter ξ_α is known as the progress variable. When the reaction has proceeded to completion to the right, $d\xi_\alpha = 1$, i.e. $\Delta\nu_{i\alpha}$ molecules of substance i have been produced.

As for the affinities, well before a practical measure of these somewhat "anthropomorphic quantities" was found (Joos), the concept of chemical affinity had been widely used. Van't Hoff first recognised that for reactions at constant V and T, the free energy F is the proper measure of affinity, while for reactions at constant p and T, the Gibb's potential G serves this purpose. These quantities are minimum at equilibrium; the greater the values of these functions compared with the minimum values, the further the system is from equilibrium, and consequently, the more readily the reaction will occur.

If only expansion work is performed on a system, all reactions then being fixed, the process is reversible. The quantity $-pdV$ is then the contribution of the external variables to dW_{rev}. If however, reactions occur at constant volume, the process is not reversible. Therefore other terms must be subtracted from $-pdV$ in order to obtain dW_{rev}. These terms will be of the form

$$\sum_{\alpha} A_{\alpha}\, d\xi_{\alpha} ,$$

where the A_{α}'s are the affinities, and the ξ_{α}'s are the progress variables. Therefore

$$d\,W_{rev} = -pdV - \sum_{\alpha} A_{\alpha}\, d\xi_{\alpha} .$$

The first law of thermodynamics thus takes the form

$$dU = d\,W_{rev} + d\,Q_{rev} = T\,dS - pdV - \sum_{\alpha} A_{\alpha}\, d\xi_{\alpha}, \qquad (1\text{-}13)$$

from which we obtain an expression for A_{α}:

$$A_{\alpha} = -\left(\frac{\partial U}{\partial \xi_{\alpha}}\right)_{VS} \qquad (1\text{-}14)$$

Just as $-p$ and T are thermodynamically conjugate to V and S respectively, $-A$ is thermodynamically conjugate to ξ_α.

Since the various thermodynamic potentials are defined by the equations

$$G = U - TS + pV$$

$$F = U - TS$$

and

$$H = U + pV,$$

the following expressions for A also hold:

$$A_\alpha = -\left(\frac{\partial G}{\partial \xi_\alpha}\right)_{pT} = -\left(\frac{\partial F}{\partial \xi_\alpha}\right)_{VT} = -\left(\frac{\partial H}{\partial \xi_\alpha}\right)_{pS} \tag{1-15}$$

where G, F, H are respectively the Gibbs free enthalpy, the Helmholtz free energy and the enthalpy.

The physical variables x and y will now be introduced. The quantity y stands for either S or T, while x stands for either V or $-p$. The conjugate variables will be expressed by X and Y. Finally P denotes the thermodynamic potential corresponding to x and y.

Equation (1-13) takes the form: $(x=V,\ X=p,\ y=S,\ Y=T)$

$$dP = -X\,dx + Y\,dy - \sum_{\alpha} A_{\alpha}\,d\xi_{\alpha} \tag{1-16}$$

while equation (1-15) becomes

$$A_{\alpha} = -\left(\frac{\partial P}{\partial \xi_{\alpha}}\right)_{xy} . \tag{1-17}$$

Differentiating A_{α} with respect to x yields:

$$\left(\frac{\partial A_{\alpha}}{\partial x}\right)_{\xi y} = -\left(\frac{\partial^2 P}{\partial \xi_{\alpha}\,\partial x}\right)_{y} = \left(\frac{\partial X}{\partial \xi_{\alpha}}\right)_{xy} \tag{1-18}$$

A few other useful formulae can be derived, and are given below.

$$\left(\frac{\partial A_{\alpha}}{\partial x}\right)_{\xi y} = -\left(\frac{\partial A_{\alpha}}{\partial \xi_{\alpha}}\right)_{xy} \left(\frac{\partial \xi_{\alpha}}{\partial x}\right)_{A_{\alpha} y} \tag{1-19a}$$

$$\left(\frac{\partial A_{\alpha}}{\partial \xi_{\alpha}}\right)_{Xy} = \left(\frac{\partial A_{\alpha}}{\partial \xi_{\alpha}}\right)_{xy} \left(\frac{\partial x}{\partial X}\right)_{\xi y} \left(\frac{\partial X}{\partial x}\right)_{A_{\alpha} y} \tag{1-19b}$$

The fundamentals of the thermodynamics of irreversible processes have been summarized in this section, following the treatment by Bauer (1965).

[illegible]

[illegible]

[illegible]

$$[illegible]$$

[illegible]

$$[illegible]$$

[illegible]

$$[illegible]$$

[illegible]

$$[illegible]$$

$$[illegible]$$

[illegible]

2. Classical Sound Absorption

Using the principles stated in the preceding section, the rate of entropy production will be determined, showing that, in the case of an isotropic fluid without reactions, the fluxes are the heat flux $\vec{J}_q$ and the pressure tensor Π, while their respective conjugated forces are the gradient of the reciprocal temperature, and the flow velocities. The phenomenological equations will then be set up, which together with the equations of continuity for mass, momentum and energy, constitute a system of homogeneous equations. When this system of equations is linearized and solved, the complex wave vector k for the sound propagation can be found. A detailed exposition for finding the wave vector k now follows.

By the principle of conservation of energy, the total energy content within an arbitrary volume V in the system can only change if energy flows into or out of the volume through its surface. With the help of Gauss' theorem, the differential form of the law of conservation of energy is obtained:

$$\frac{\partial \rho e}{\partial t} = -\nabla \cdot \vec{J}_e \, , \qquad (1\text{-}25)$$

where ρ is the density, e is the total energy per unit mass and $\vec{J}_e$ the total energy flux per unit surface and unit time. Here e includes all forms of energy in the system and may be written in the form,

$$e = \frac{1}{2} v^2 + u, \tag{1-26}$$

where $\frac{1}{2} v^2$ is the specific kinetic energy, and u is the specific internal energy. Similarly $\vec{J}_e$ includes all forms of energy fluxes: a convective term $\rho e\vec{v}$, an energy flux $\Pi\cdot\vec{v}$ due to the mechanical work performed on the system, and finally, the heat flux $\vec{J}_q$:

$$\vec{J}_e = \rho e\vec{v} + \Pi\cdot\vec{v} + \vec{J}_q \quad . \tag{1-27}$$

The conservation law for energy of a fluid in the absence of external forces can thus be written:

$$\rho \frac{de}{dt} = - \nabla \cdot (\Pi\cdot\vec{v} + \vec{J}_q) \tag{1-28}$$

where

$$\frac{d}{dt} = \frac{\partial}{\partial t} + \vec{v} \cdot \nabla \tag{1-29}$$

is the so-called differential following the motion.

Remembering that in a fluid, only differences of pressure give rise to a force (constant, normal or shearing stresses do not produce a force) the conservation law of momentum can be written as

$$\rho \frac{d\vec{v}}{dt} = - \nabla \cdot \Pi \quad . \tag{1-30}$$

Combining equations (1-26) and (1-28) gives the balance of internal energy.

$$\rho \frac{du}{dt} = - \Pi : \nabla \vec{v} - \nabla \cdot \vec{J}_q \tag{1-31}$$

It is now useful to split the pressure tensor into two parts: the hydrostatic pressure p, and the symmetric viscous pressure tensor Π_s. This is justified, since the components of the stress tensor are the following:

$$\Pi_{ii} = p - 2\eta\left(\frac{\partial v_i}{\partial r_i} - \frac{1}{3}\nabla \cdot \vec{v}\right) \tag{1-32a}$$

$$\Pi_{ij} = \eta\left(\frac{\partial v_i}{\partial r_j} + \frac{\partial v_j}{\partial r_i}\right) \tag{1-32b}$$

where $r_i, r_j = x,y,z$

$v_i, v_j = v_x, v_y, v_z$

and η is the shear viscosity. For a monatomic gas, the bulk viscosity is identically equal to zero. The hydrostatic pressure

$$p = \frac{1}{3}\left(\Pi_{xx} + \Pi_{yy} + \Pi_{zz}\right). \tag{1-33}$$

The balance equation for the internal energy and the law of conservation of mass become respectively:

$$\rho \frac{du}{dt} = - p \nabla \cdot \vec{v} - \Pi_s : \nabla \vec{v} - \nabla \cdot \vec{J}_q \quad , \tag{1-34}$$

and

$$\rho \frac{dV}{dt} = \nabla \cdot \vec{v} \ . \qquad (V \equiv \rho^{-1}) \tag{1-35}$$

From the last two equations,

$$\rho\left(\frac{du}{dt} + p \frac{dV}{dt}\right) = -\Pi_s : \nabla \vec{v} - \nabla \cdot \vec{J}_q \tag{1-36}$$

which can be inserted into the Gibbs relation:

$$T \frac{dS}{dt} = \frac{du}{dt} + p \frac{dV}{dt} \tag{1-37}$$

Thus the entropy balance equation is obtained:

$$\rho \frac{dS}{dt} = -\nabla \cdot \vec{J}_s + \sigma \tag{1-38}$$

with the entropy flow

$$\vec{J}_s = \frac{\vec{J}_q}{T} \tag{1-39}$$

and the entropy production

$$\sigma = -\vec{J_q} \cdot \frac{\nabla(T)}{T^2} - \frac{\Pi_s : \nabla \vec{v}}{T} \geqslant 0 \qquad (1\text{-}40)$$

As mentioned before, the entropy production is a sum of products of fluxes and thermodynamic forces, the former being related to the latter through the phenomenological equations (1-7). Since the phenomenological coefficients can be temperature dependent, new coefficients can now be introduced into which such factors as $\frac{1}{T}$ and $\frac{1}{T^2}$ can be absorbed.

The familiar expression

$$\vec{J}_q = - \varphi \nabla T, \qquad (1\text{-}41)$$

where φ is the heat conductivity, is obtained through such simple considerations, from equation (1-40). Similarly, equations (1-32) yield in turn

$$\Pi_s = -2\eta\left(\nabla \vec{v} - \frac{1}{3} \nabla \cdot \vec{v}\, U\right), \qquad (1\text{-}42)$$

where U is a unit tensor.

The present treatment follows in broad outline and is a simplification of the treatment by De Groot and Mazur[2], but will henceforth be restricted to one dimension. In such a case, the laws of conservation of mass and momentum are

$$\frac{d\rho}{dt} + \rho \frac{\partial v_x}{\partial x} = 0 \qquad (1\text{-}43)$$

and

$$\rho \frac{dv_x}{dt} + \frac{\partial p}{\partial x} - \frac{4}{3}\eta \frac{\partial^2 v_x}{\partial x^2} = 0 \qquad (1\text{-}44)$$

Again, restricting the problem to one-dimension, and inserting the phenomenological equations (1-41), (1-42) into the energy law (1-34), the following expression is obtained:

$$\rho \frac{du}{dt} + p \frac{\partial v_x}{\partial x} - \frac{4}{3}\eta \left(\frac{\partial v_x}{\partial x}\right)^2 - \varphi \frac{\partial^2 T}{\partial x^2} = 0 \qquad (1\text{-}45)$$

Now it is well known that for a monatomic gas whose molecules possess translational kinetic energy only, the internal energy of the gas equals $\frac{3}{2}$ kT. Moreover, from the equation of state of the gas (k is Boltzmann's constant)

$$T = \frac{p}{\rho} \left(\frac{m}{k}\right) \qquad (1\text{-}46)$$

where m is the mass of a molecule of the gas. Therefore the internal energy per unit mass becomes

$$u = \frac{3}{2}\frac{p}{\rho} \quad . \tag{1-47}$$

The three preceding equations have to be linearized, in order to handle them easily mathematically. In the case of moderately weak ultrasonic waves, the usual procedure for linearizing these equations is to express ρ and p as

$$\rho = \rho_0 (1 + \epsilon) \quad , \quad p = p_0 (1 + \delta) \ . \tag{1-48}$$

Here ρ_0 and p_0 are respectively the density and the pressure of the fluid in the absence of perturbation. ϵ and δ are small compared to unity, while $\vec{v}$ the flow velocity is very much smaller than the sound velocity. Therefore, powers higher than one and products of these quantities or of their derivatives, can be neglected. Substituting for ρ , p and u, equations (1-43), (1-44) and (1-45) become:

$$\frac{\partial \epsilon}{\partial t} + \frac{\partial v_x}{\partial x} = 0 \tag{1-49}$$

$$\frac{\partial v_x}{\partial t} + \frac{p_0}{\rho_0}\frac{\partial \delta}{\partial x} - \frac{4}{3}\frac{\eta}{\rho_0}\frac{\partial^2 v_x}{\partial x^2} = 0 \quad \text{and} \tag{1-50}$$

$$\frac{3}{2}\frac{\partial}{\partial t}(\delta - \epsilon) + \frac{\partial v_x}{\partial x} - \frac{\varphi}{\rho_0 k}\frac{\partial^2}{\partial x^2}(\delta - \epsilon) = 0 \quad . \tag{1-51}$$

Eliminating v_x from the above equations, there results

$$\frac{p_0}{\rho_0} \frac{\partial^2 \delta}{\partial x^2} - \frac{\partial^2 \epsilon}{\partial t^2} + \frac{4}{3} \frac{\eta}{\rho_0} \frac{\partial^3 \epsilon}{\partial x^2 \partial t} = 0 \qquad (1\text{-}52)$$

and

$$\frac{\partial \delta}{\partial t} - \frac{5}{3} \frac{\partial \epsilon}{\partial t} - \frac{2}{3} \left(\frac{\varphi}{\rho_0 k} \right) \frac{\partial^2}{\partial x^2} (\delta - \epsilon) = 0 \qquad (1\text{-}53)$$

Equations (1-52) and (1-53) are the equations governing the propagation of sound waves of small amplitude in a gas treated as a continuous medium. Assuming that the sound wave is propagated as a damped progressive wave, ϵ and δ must be of the form

$$\epsilon = \epsilon_0 e^{i(Kx - \omega t)} \quad \text{and} \quad \delta = \delta_0 e^{i(Kx - \omega t)} .$$

Substituting these values into equations (1-52), (1-53) yields two homogeneous equations for ϵ_0 and δ_0.

$$\epsilon_0 \left(\omega^2 + i \frac{4}{3} \frac{\eta}{\rho_0} \omega K^2 \right) - K^2 \frac{p_0}{\rho_0} \delta_0 = 0 \qquad (1\text{-}54)$$

$$\epsilon_0 \left(\frac{5}{3} + i \frac{2}{3} \frac{\varphi}{\rho_0} \frac{K^2}{k\omega} \right) + \delta_0 \left(-i \frac{2}{3} \frac{\varphi}{\rho_0} \frac{K^2}{k} - 1 \right) = 0 \qquad (1\text{-}55)$$

Since the determinant of these equations must be zero for consistency, we obtain a quadratic equation in K^2, namely

$$K^4\left[-\frac{8}{9}\frac{\eta}{\rho_0^2}\frac{\omega}{k} + i\,\frac{2}{3}\frac{\varphi}{\rho_0}\frac{p_0}{k\omega}\right] + K^2\left[\frac{5}{3}\frac{p_0}{\rho_0} + i\,\frac{\omega^2\varphi}{3\rho_0 k} + i\,\frac{4}{3}\frac{\eta}{\rho_0}\omega\right] + \omega^2 = 0 \qquad (1\text{-}56)$$

An approximation to the classical sound absorption coefficient α_{class}, which is often encountered in the literature can be derived from equation (1-56) by means of various substitutions. Firstly $V_0 = \left(\frac{5}{3}\frac{p_0}{\rho_0}\right)^{1/2}$ is the adiabatic sound velocity at low frequencies for a monatomic gas. Next let $k_i = \frac{K}{\beta_0} = \frac{K\,V_0}{\omega}$ and $\varphi = \frac{15}{4}\,k$. Further, following Greenspan[3] let $R = \frac{\rho_0 V_0^2}{\eta\,\omega}$ where R is the Reynold's number taken from the field of gas dynamics. Equation (1-56) becomes

$$k_i^4\left[\frac{3}{2}\frac{i}{R} - \frac{10}{3}\frac{1}{R^2}\right] + k_i^2\left[1 + \frac{23}{6}\frac{i}{R}\right] + 1 = 0$$

or $$k_i^2 = R\,\frac{R + \frac{23}{6}i - \left(R^2 - \frac{49}{36} + \frac{5}{3}iR\right)^{1/2}}{\frac{20}{3} - 3iR}$$

Thus $$k_i = i + \frac{7}{6}\frac{1}{R} - \frac{141}{72}\frac{i}{R^2} - \frac{1559}{432}\frac{1}{R^3} + \cdots \qquad (1\text{-}57)$$

which is obtained from the preceding equation by series approximation.

In the zeroth approximation, the velocity is constant, and there is no attenuation. The first approximation gives the "classical" attenuation per unit length

$$\frac{\alpha \text{ class}}{\beta_0} = \frac{\alpha \text{ class} \lambda_0}{2\pi} = \frac{7}{6}\frac{1}{R}, \qquad (1\text{-}58)$$

where λ_0 is the wave-length at low frequencies. Equation (1-58) can be shown to be equivalent to the usual approximation:

$$\alpha_{class} = \frac{2\pi^2}{\gamma p_0 V_0}\left[\frac{4}{3}\eta + \frac{\gamma-1}{C_p}\varphi\right]f^2 \qquad (1\text{-}59)$$

Here C_p is the specific heat at constant pressure, γ is the ratio of the specific heats and f is the number of vibrations per unit time of the sound wave.

Indeed the equivalence of (1-58), (1-59) follows easily, since $\gamma = \frac{5}{3}$ in the case of a monatomic gas and $\lambda = \frac{5}{2}\eta C_v$ by the kinetic theory of gases, where C_v is the specific heat at constant volume. Thus the classical sound absorption is seen from (1-59), to be directly proportional to the square of the frequency, and inversely proportional to the pressure.

3. Relaxational Absorption

When a fluid is given a periodic deformation, as is the case when a sound wave is transmitted through the fluid, a phase lag exists between the stresses and the strains, which is responsible for the absorption of sound. In monatomic gases, this phase lag is due entirely to viscosity and heat conduction. In diatomic and polyatomic gases however, the absorption of sound is also due to the failure of the internal degrees of freedom to remain in thermal equilibrium with the external degrees of freedom. The process by which the temperature of the internal degrees of freedom adjusts itself to the temperature of the external degrees of freedom is a typical relaxation process. Due to the passage of the sound wave, the "translational temperature" is increased. In order to be again in equilibrium with the new translational energy, the internal energy must also increase; i.e. energy must flow from the translational to the internal degrees of freedom. This can only occur through collisions, and takes a finite time. The time needed to decrease the maladjustment by a factor e^{-1} is called the relaxation time. Such a process is called a reaction in the language of the thermodynamics of irreversible processes and the value of the relaxation time depends on whether the reaction proceeds isothermally or adiabatically.

Again, following Bauer (1965), the phenomenological equations are easily set up as follows. Combining equations (1-3), (1-5) and (1-13) yields the rate of entropy production,

$$\sigma = \frac{1}{T} \sum A_\alpha \dot{\xi}_\alpha \quad .$$

After absorbing the factor $\frac{1}{T}$ into the phenomenological coefficients, the phenomenological equations become:

$$\dot{\xi}_\alpha = \sum_\beta L_{\alpha\beta} A_\beta \qquad (\alpha = 1, \ldots, r). \qquad (1\text{-}60)$$

In the case of a single relaxation process, equation (1-60) takes the form:

$$\dot{\xi} = LA \quad . \qquad (1\text{-}61)$$

L may be assumed to be constant within a small region. However A depends on the variables $x(\equiv V \text{ or } -p)$, $y(\equiv S \text{ or } T)$ and ξ. Within a small region about the point (x_0, y_0, ξ_0):

$$A(x,y,\xi) = A(x_0,y_0,\xi_0) + \left(\frac{\partial A}{\partial \xi}\right)_{xy} (\xi - \xi_0) + \left(\frac{\partial A}{\partial x}\right)_{\xi y} (x - x_0) + \left(\frac{\partial A}{\partial y}\right)_{\xi x} (y - y_0) \quad . \qquad (1\text{-}62)$$

If the point (x_0, y_0, ξ_0) is an equilibrium point, $A(x_0, y_0, \xi_0)$ vanishes, since as stated earlier, the affinities vanish at equilibrium. From equations (1-60), (1-61) the so-called relaxation equation (1-62) is obtained.

$$\dot{\xi} = L\left[\left(\frac{\partial A}{\partial \xi}\right)_{xy}(\xi-\xi_0) + \left(\frac{\partial A}{\partial x}\right)_{\xi,y}(x-x_0) + \left(\frac{\partial A}{\partial y}\right)_{\xi,x}(y-y_0)\right] \tag{1-63}$$

Moreover by holding the external variables x and y constant at $x = x_0$, $y = y_0$ the last equation becomes a linear homogeneous differential equation whose solution is

$$(\xi - \xi_0) = (\xi_{t=0} - \xi_0)\exp\left(-\frac{t}{\tau_{xy}}\right) \tag{1-64}$$

with the reciprocal relaxation time

$$\frac{1}{\tau_{xy}} = -L\left(\frac{\partial A}{\partial \xi}\right)_{xy} \quad . \tag{1-65}$$

If the experiment is performed under different conditions, so that X and y are kept constant, rather than x and y, a different relaxation time τ_{Xy} will result. The relation between these various relaxation times is given by equations (1-65) and (1-19b)

$$\frac{\tau_{xy}}{\tau_{Xy}} = \left(\frac{\partial A}{\partial \xi}\right)_{Xy} \Big/ \left(\frac{\partial A}{\partial \xi}\right)_{xy} = \left(\frac{\partial x}{\partial X}\right)_{\xi y} \left(\frac{\partial X}{\partial x}\right)_{Ay}$$

the operator $\left(\frac{\partial}{\partial x}\right)_{Ay}$ represents the differentiation carried out during equilibrium, while the operator $\left(\frac{\partial}{\partial x}\right)_{\xi y}$ represents the differentiation carried out during an arrested reaction. The values obtained by means of these operators are often referred to as quasi-static and instantaneous or frozen-in values respectively.

For the four variables p, V, T and S, the various relaxation times are related as follows:

$$\frac{\tau_{pT}}{\tau_{VT}} = \left(\frac{\partial A}{\partial \xi}\right)_{VT} \Big/ \left(\frac{\partial A}{\partial \xi}\right)_{pT} = \left(\frac{\partial V}{\partial p}\right)_{AT} \left(\frac{\partial p}{\partial V}\right)_{\xi T} = K_T^{o} \Big/ K_T^{\infty} \quad , \qquad (1\text{-}66)$$

$$\frac{\tau_{pT}}{\tau_{pS}} = \left(\frac{\partial A}{\partial \xi}\right)_{pS} \Big/ \left(\frac{\partial A}{\partial \xi}\right)_{pT} = \left(\frac{\partial S}{\partial T}\right)_{Ap} \left(\frac{\partial T}{\partial S}\right)_{\xi p} = C_p^{o} \Big/ C_p^{\infty} \quad , \qquad (1\text{-}67)$$

$$\frac{\tau_{VT}}{\tau_{VS}} = \left(\frac{\partial A}{\partial \xi}\right)_{VS} \Big/ \left(\frac{\partial A}{\partial \xi}\right)_{VT} = \left(\frac{\partial S}{\partial T}\right)_{AV} \left(\frac{\partial T}{\partial S}\right)_{\xi V} = C_V^{o} \Big/ C_V^{\infty} \quad , \qquad (1\text{-}68)$$

$$\frac{\tau_{pS}}{\tau_{VS}} = \left(\frac{\partial A}{\partial \xi}\right)_{VS} \Big/ \left(\frac{\partial A}{\partial \xi}\right)_{pS} = \left(\frac{\partial V}{\partial p}\right)_{AS} \left(\frac{\partial p}{\partial V}\right)_{\xi S} = K_S^{o} \Big/ K_S^{\infty} \quad . \qquad (1\text{-}69)$$

K_T and K_S are the isothermal and the adiabatic compressibilities respectively. The indices o and ∞ refer to the quasi-static and instantaneous values respectively.

Unfortunately, the progress variables cannot be observed themselves, and the relaxation times cannot be determined as easily as equation (1-64) seems to indicate. They can only be found from the behaviour of another dependent variable z, which is a function of x, y and ξ. Therefore, if instead of being kept constant, x and y are allowed to vary, with the help of (1-65) and (1-19a), equation (1-63) becomes:

$$\dot{\xi} = -\frac{1}{\tau_{xy}}\left[(\xi-\xi_0) - \left(\frac{\partial \xi}{\partial x}\right)_{Ay}(x-x_0) - \left(\frac{\partial \xi}{\partial y}\right)_{Ax}(y-y_0)\right] \tag{1-70}$$

On the other hand $z = z(x,y,\xi)$ can be expanded linearly about x_0, y_0, ξ_0 as follows:

$$z - z_0 = \left(\frac{\partial z}{\partial \xi}\right)_{xy}(\xi-\xi_0) + \left(\frac{\partial z}{\partial x}\right)_{\xi y}(x-x_0) + \left(\frac{\partial z}{\partial y}\right)_{\xi x}(y-y_0) \tag{1-71}$$

$\xi, \dot{\xi}$ can be eliminated from the last two equations, yielding

$$\left[1+\tau_{xy}\frac{d}{dt}\right](z-z_0) = \left[\left(\frac{\partial z}{\partial \xi}\right)_{xy}\left(\frac{\partial \xi}{\partial x}\right)_{Ay} + \left(\frac{\partial z}{\partial x}\right)_{\xi y}\left(1+\tau_{xy}\frac{d}{dt}\right)\right](x-x_0)$$

$$+\left[\left(\frac{\partial z}{\partial \xi}\right)_{xy}\left(\frac{\partial \xi}{\partial y}\right)_{Ax} + \left(\frac{\partial z}{\partial y}\right)_{\xi x}\left(1+\tau_{xy}\frac{d}{dt}\right)\right](y-y_0) \tag{1-72}$$

From equation (1-19b), it follows that

$$\left(\frac{\partial z}{\partial \xi}\right)_{xy}\left(\frac{\partial \xi}{\partial x}\right)_{Ay} = \left(\frac{\partial z}{\partial x}\right)_{Ay} - \left(\frac{\partial z}{\partial x}\right)_{\xi y} ,$$

and that

$$\left(\frac{\partial z}{\partial \xi}\right)_{xy}\left(\frac{\partial \xi}{\partial y}\right)_{Ax} = \left(\frac{\partial z}{\partial y}\right)_{Ax} - \left(\frac{\partial z}{\partial x}\right)_{\xi y} .$$

Equation (1-72) now becomes:

$$\left[1 + \tau_{xy}\frac{d}{dt}\right](z - z_o) = \left[\left(\frac{\partial z}{\partial x}\right)_{Ay} + \left(\frac{\partial z}{\partial x}\right)_{\xi y}\tau_{xy}\frac{d}{dt}\right](x - x_o) \qquad (1\text{-}73)$$
$$+ \left[\left(\frac{\partial z}{\partial y}\right)_{Ax} + \left(\frac{\partial z}{\partial y}\right)_{\xi x}\tau_{xy}\frac{d}{dt}\right](y - y_o) .$$

Assuming that the state variables are of the form:

$$(x - x_o) = C e^{j(\omega t + d)} ,$$

the differential operator $\frac{d}{dt}$ is simply $j\omega$. Thus equation (1-73) takes on the form

$$(z - z_o) = \left[\left(\frac{\partial z}{\partial x}\right)_{Ay} + j\omega\,\tau_{xy}\left(\frac{\partial z}{\partial x}\right)_{\xi y}(x - x_o) + \left(\frac{\partial z}{\partial y}\right)_{Ax} + j\omega\,\tau_{xy}\left(\frac{\partial z}{\partial y}\right)_{\xi x}(y - y_o)\right] \Big/ (1 + j\omega\,\tau_{xy})$$

or

$$(z - z_0) = \left(\frac{\partial z}{\partial x}\right)_y^{eff} (x - x_0) + \left(\frac{\partial z}{\partial y}\right)_x^{eff} (y - y_0) ,$$

where

$$\left(\frac{\partial z}{\partial x}\right)_y^{eff} = \left(\frac{\partial z}{\partial x}\right)_{Ay} \frac{1 + j\omega\hat{\tau}_{yz}}{1 + j\omega\hat{\tau}_{xy}} \qquad (1\text{-}74a)$$

and

$$\left(\frac{\partial z}{\partial y}\right)_x^{eff} = \left(\frac{\partial z}{\partial y}\right)_{Ax} \frac{1 + j\omega\hat{\tau}_{xz}}{1 + j\omega\hat{\tau}_{xy}} . \qquad (1\text{-}74b)$$

The derivatives $\left(\frac{\partial z}{\partial x}\right)_y^{eff}$ and $\left(\frac{\partial z}{\partial y}\right)_x^{eff}$ are clearly the effective state coefficients, which take into account the finite reaction rates. These equations can now be applied to the case of acoustic relaxation.

If we neglect the transport phenomena, the adiabatic character of the process is guaranteed. In the absence of the dissipative factors, the equations of continuity for momentum, mass and energy yield the Laplacian formula for the wave-vector k_o :

$$\frac{k_o^{2}}{\omega^2} = K_S^{o}\rho = \frac{1}{c_o^{2}} \qquad (1\text{-}75)$$

where K_S^{o} is the adiabatic compressibility, in the absence of relaxation. If the internal transitions are now taken into account, the adiabatic compressibility must be replaced by an effective adiabatic compressibility K_S^{eff}. K_S^{eff} can be easily found in terms of τ_{yz} and τ_{xy}. To do this the following choice of variables is made:

$$x \equiv -p, \quad y \equiv S \equiv S_o, \quad z = \rho = \frac{M}{V} \ .$$

Using equation (1-74) with

$$\frac{1}{\rho}\left(\frac{\partial \rho}{\partial p}\right)_s = -\frac{1}{V}\left(\frac{\partial V}{\partial p}\right)_s = K_s \qquad \text{and} \qquad \tau_{\rho s} \equiv \tau_{Vs} \ ,$$

a "normalized" effective adiabatic compressibility is obtained:

$$\frac{K_S^{eff}}{K_S^{o}} = \frac{1 + j\omega \tau_{Vs}}{1 + j\omega \tau_{\rho s}} \ .$$

The locus of K_S^{eff}/K_S^{o} can be obtained by means of the conformal mapping $w = \frac{z + j\tau_{Vs}}{z + j\tau_{\rho s}}$ onto the positive real axis $z = 1/\omega$. This gives a semi-circle of diameter $\epsilon = 1 - \frac{\tau_{Vs}}{\tau_{\rho s}}$. ϵ is called the relaxation strength. The maximum of the imaginary part occurs when $\omega = \frac{1}{\tau_{\rho s}}$. This locus, which is known as the Cole plot, is useful in determining

whether sound absorption or dispersion is due to a single relaxation process or to a multiple relaxation process: the curve is a semi-circle in the former case only.

Under these conditions, equation (1-75) must be replaced by:

$$\frac{k_r^2}{\omega^2} = K_S^{eff} \rho \tag{1-76}$$

where k_r is the complex wave vector

$$k_r = \frac{\omega}{C} - j \alpha' \quad . \tag{1-77}$$

If the value of k_r given by (1-77) is substituted into (1-76), and both sides are multiplied by $C_o^2 = \frac{1}{\rho K_s^o}$ an obvious simplification yields

$$\begin{aligned} \frac{C_o^2}{C^2} - \frac{\alpha' C_o^2}{\omega^2} - j \frac{2\alpha' C_o^2}{\omega C} &= \frac{K^{eff}}{K_s^o} \\ &= \frac{1 + \omega^2 \tau_{vs} \tau_{ps}}{1 + \omega^2 \tau_{ps}^2} - j \frac{\omega(\tau_{ps} - \tau_{vs})}{1 + \omega^2 \tau_{ps}^2} \quad . \end{aligned} \tag{1-78}$$

The real and imaginary parts of (1-78) will be equated separately in what follows. Comparing first the real part,

$$\frac{C_o^2}{C^2} - \frac{\alpha' C_o^2}{\omega^2} = \frac{1 + \omega^2 \tau_{ps} \tau_{vs}}{1 + \omega^2 \tau_{ps}^2} \tag{1-79}$$

Now, C_o is not very different from C. Thus $\frac{\alpha' C_o^2}{\omega^2}$ may also be written as $\frac{\alpha' C_o^2}{\omega^2} = \frac{\alpha' \lambda^2}{4\pi^2}$, where λ is the wavelength of the sound wave. Moreover, in most cases $(\alpha'\lambda)^2 / 4\pi^2 \ll 1$. Under these conditions, (1-79) can be approximated by

$$\frac{C_o^2}{C^2} = \frac{1 + \omega^2 \tau_{VS} \tau_{pS}}{1 + \omega^2 \tau^2_{pS}} .$$

However, from (1-66)

$$\tau_{VS}\tau_{pS} = \tau^2_{pS} \frac{K_S^\infty}{K_S^o} = \tau^2_{pS} (1 - \epsilon) ,$$

so that finally

$$\frac{C_o^2}{C^2} = 1 - \frac{\epsilon \omega^2 \tau^2_{pS}}{1 + \omega^2 \tau^2_{pS}} . \tag{1-80}$$

Plotted on a logarithmic frequency scale, this function exhibits a dispersion step with an inflection point at

$\omega = \frac{1}{\tau_{pS}}$.

If on the other hand, the imaginary parts of (1-78) are compared, it is easily seen that

$$2 \frac{\alpha' C_a^2}{\omega C} = \frac{\alpha' \lambda}{\pi} \frac{C_o^2}{C^2} = \frac{\omega (\tau_{pS} - \tau_{VS})}{1 + \omega^2 \tau^2_{pS}}$$

$\alpha' \lambda$ is called the molecular absorption index, and is designated by μ or α_λ. Using (1-80) a little simplification yields:

$$\mu \frac{C_o^2}{C^2} = \pi \epsilon \frac{\omega \tau_{pS}}{1+\omega^2 \tau_{pS}^2} \tag{1-81}$$

and

$$\mu = \alpha' \lambda = \frac{\pi \epsilon}{\sqrt{1-\epsilon}} \cdot \omega \frac{\sqrt{\tau_{pS} \tau_{vS}}}{1+\omega^2 \tau_{pS} \tau_{vS}} . \tag{1-82}$$

When plotted against $\ln \omega$, both $\mu \frac{C_o^2}{C^2}$ and μ are bell-shaped curves. The maxima of these curves are at $\omega = \frac{1}{\tau_{pS}}$ and $\omega = \frac{1}{\sqrt{\tau_{pS} \tau_{vS}}}$ respectively.

The curves of $\frac{C_o^2}{C^2}$, $\mu \frac{C_o^2}{C^2}$ and μ appear in fig. (1) a), b) and c) respectively.

Acoustic measurements can therefore yield the values of τ_{pS} and τ_{VS}. Equation (1-81) in particular constitutes the basis for the measurements reported in this thesis; the molecular absorption index is thus seen to be related to the two adiabatic relaxation time τ_{pS} and τ_{VS}.

On the other hand the relaxation times can be calculated by means of equations (1-65). However, the thermodynamics of irreversible processes does not provide any information about the progress variables or about the affinities. Reaction

Fig. 1

a) $(C_o/C)^2$ vs $\ln \omega$

b) $\mu\ (C_o/C)^2$ vs $\ln \omega$

c) μ vs $\ln \omega$

(a)

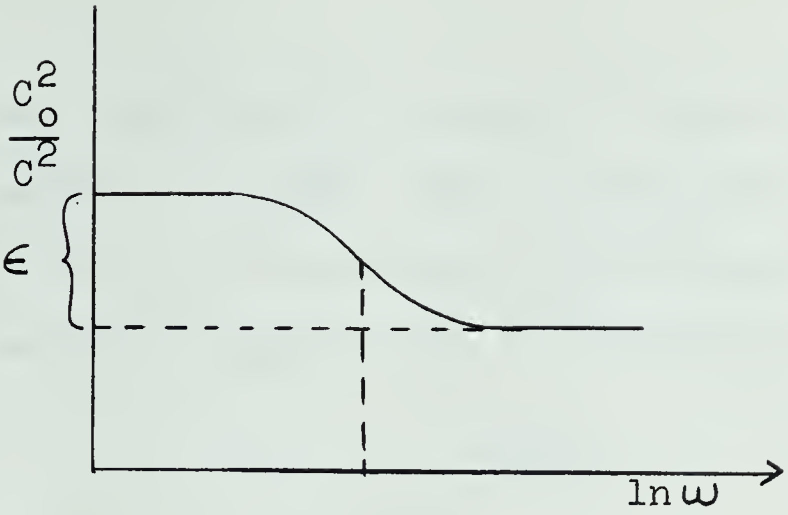
$\frac{C_o^2}{C^2}$
ϵ
ln ω

(b)

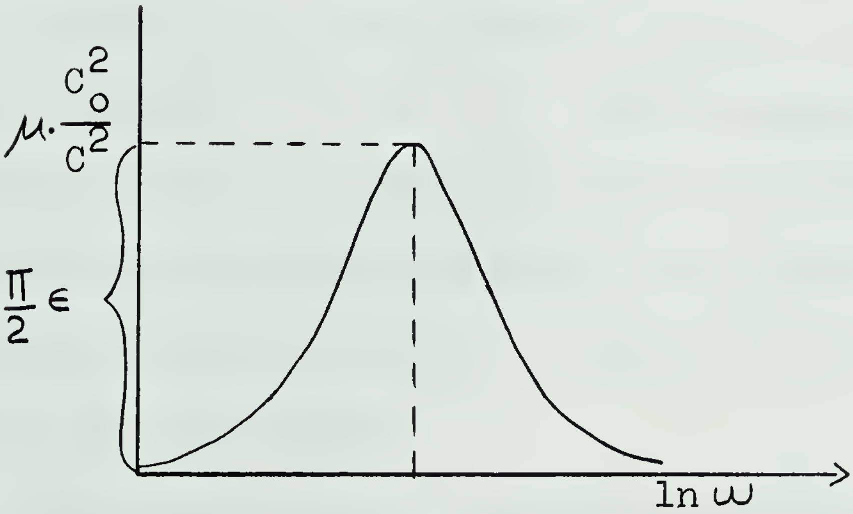
$\mu \cdot \frac{C_o^2}{C^2}$
$\frac{\pi}{2}\epsilon$
ln ω

(c)

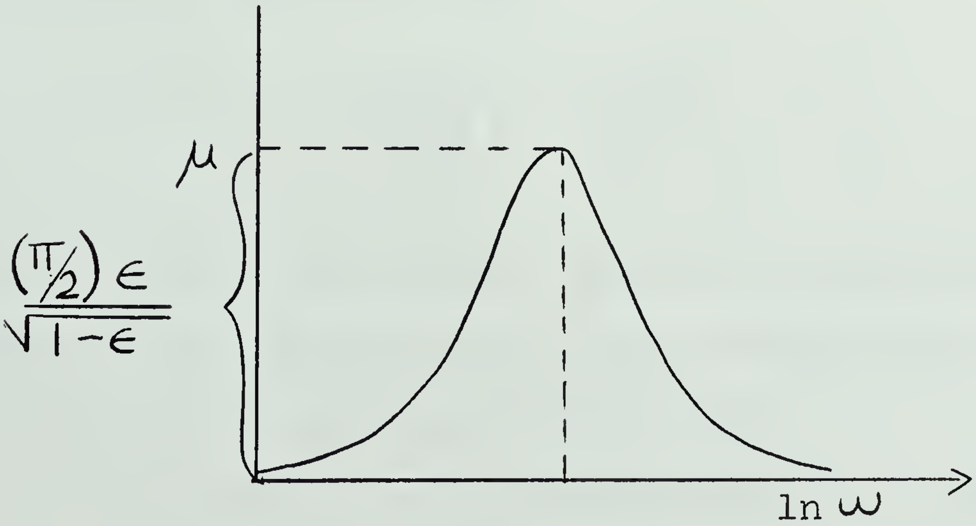
μ
$\frac{(\pi/2)\epsilon}{\sqrt{1-\epsilon}}$
ln ω

kinetics must therefore be applied in order to evaluate these parameters. For the sake of simplicity and following Kneser[4] τ will be calculated only for the special case where the reaction equation has the following form:

$$A + A_1 \rightleftharpoons A + A_o \; . \qquad (1\text{-}83)$$

This equation describes the de-excitation and excitation of internal degrees of freedom by binary collisions. A_o denotes the unexcited molecule and A represents the collision partner (A_o or A_1) which remains unchanged during the collision. Although equation (1-83) is only one of the several reactions which are possible in principle, it is the only reaction which occurs as the result of collisions in a two level gas.

The population of the ground state and that of the excited state change, during the reaction to the right, according to the equation:

$$\frac{d\,\overrightarrow{n_o}}{dt} = -\frac{d\,\overrightarrow{n_1}}{dt} = Rn_1$$

where n_o and n_1 are the number of molelecules per unit volume in the ground and in the excited states respectively; R is the rate constant to the right.

A similar equation describes the reaction to the left:

$$\frac{d\overleftarrow{n}_1}{dt} = - \frac{d\overleftarrow{n}_o}{dt} = R'n_o$$

Here R' is the rate constant to the left. If the molar number n_o is introduced as the progress variable ξ , the time derivative $\dot{\xi}$ includes $\frac{d\overrightarrow{n}_o}{dt}$ and $\frac{d\overleftarrow{n}_o}{dt}$. $\dot{\xi}$ can be expressed by

$$\dot{\xi} = Rn_1 - R'n_o = Rn_1\left(1 - \frac{n_o/n_1}{R/R'}\right) \quad . \qquad (1\text{-}84)$$

At equilibrium, $\dot{\xi} = 0$ and $n_{oo}/n_{1o} = R/R'$ where the additional subscript o (on the n's) denotes the equilibrium values. At small displacements

$$\frac{n_o}{n_1} = \frac{n_{oo} + \Delta n_o}{n_{1o} + \Delta n_1} = \frac{n_{oo} + (\xi - \xi_o)}{n_{1o} - (\xi - \xi_o)} = \frac{n_{oo}}{n_{1o}}\left[1 + \left(\frac{1}{n_{oo}} + \frac{1}{n_{1o}}\right)(\xi - \xi_o)\right].$$

This value substituted into (1-84) yields

$$\dot{\xi} = - Rn_1\left(\frac{1}{n_{oo}} + \frac{1}{n_{1o}}\right)(\xi - \xi_o) = - R\left(1 + \frac{n_{1o}}{n_{oo}}\right)(\xi - \xi_o) \quad . \qquad (1\text{-}85)$$

When the experiment is conducted under isothermal conditions, ξ_o remains constant during the relaxation process. The solution of (1-85) is then

$$(\xi - \xi_o) = (\xi_{t=o} - \xi_o)\, e^{-t/\tau_T}$$

with an isothermal relaxation time given by

$$\tau_T^{-1} = R\left(1 + \frac{n_{1o}}{n_{oo}}\right) = (R + R') \quad . \qquad (1\text{-}86)$$

When the reaction represents the excitation or the de-excitation of a molecule, the rate constants R and R' are simply proportional to the probabilities f_{o1} and f_{1o}:

$$R = \tau_c^{-1}\; f_{1o} \quad , \quad R' = \tau_c^{-1}\; f_{o1}$$

where τ_c is the mean collision time; f_{1o} is the probability that an excited molecule will return to the ground state when colliding with another one, while f_{o1} is the probability that a molecule in the ground state will be excited when colliding with another molecule. Equation (1-86) shows that the isothermal relaxation time is inversely proportional to the sum of the rate constants.

The experimental values of the sound absorption or of the velocity dispersion yield the adiabatic relaxation times τ_{pS} and τ_{VS} , while reaction kinetics calculations yield the isothermal relaxation times τ_{pT} or τ_{VT} . In order to compare the experimental values with the theoretical

values, the former must be converted into isothermal values by means of equations (1-67) and (1-68). The difference between the isothermal and the adiabatic relaxation times is often minimal, especially in the case of vibrational relaxation. It is not so however in the case of rotational relaxation. The various relaxation times are clearly indicated on fig. (2).

The following inequalities always hold:

$$\tau_{pT} > \tau_{pS} > \tau_{VS} \quad .$$

This distinction between the various relaxation times has often been ignored in the literature. Nowhere has it been expressed more clearly however, than in the papers by Bauer[1] and by Kneser.[4]

4. Relaxational Absorption in Hydrogen.

In order to compare experimental results with theoretical calculations, it is best to effect measurements on a simple molecule. Limiting ourselves to the problem of rotational energy transfer, the hydrogen molecule at low temperature constitutes such a simple model for the following reasons:

Fig. 2

a) τ_{pT}

b) τ_{pS}

c) τ_{VS}

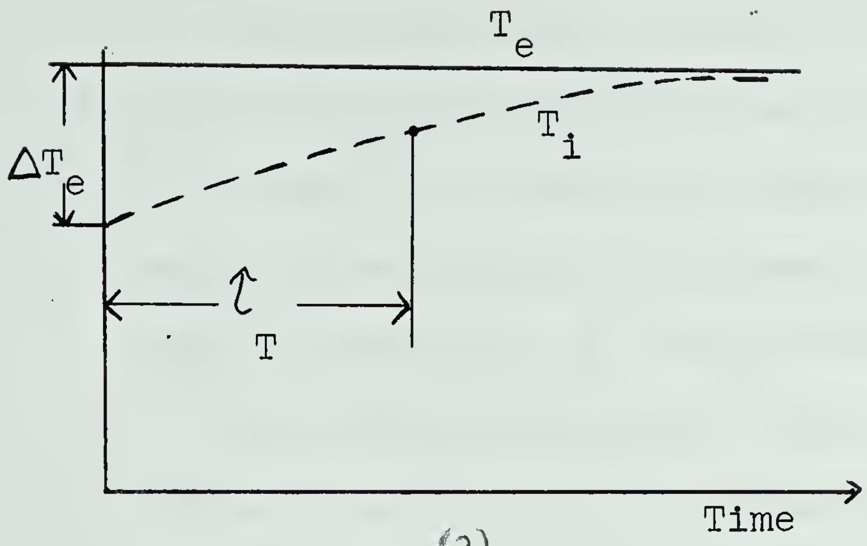
T_e
T_i
ΔT_e
τ_T
Time

T_e: external temperature

T_i: internal temperature

(a)

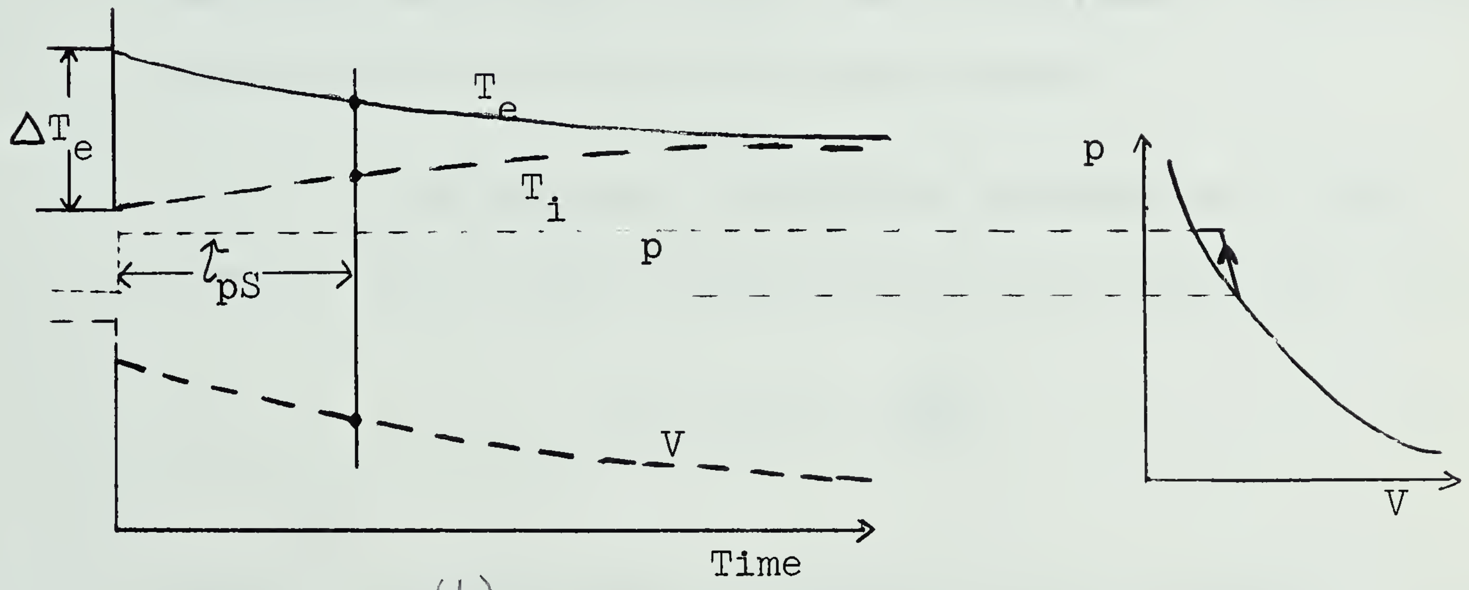
ΔT_e
T_e
T_i
τ_{pS}
p
V
Time
p
V

(b)

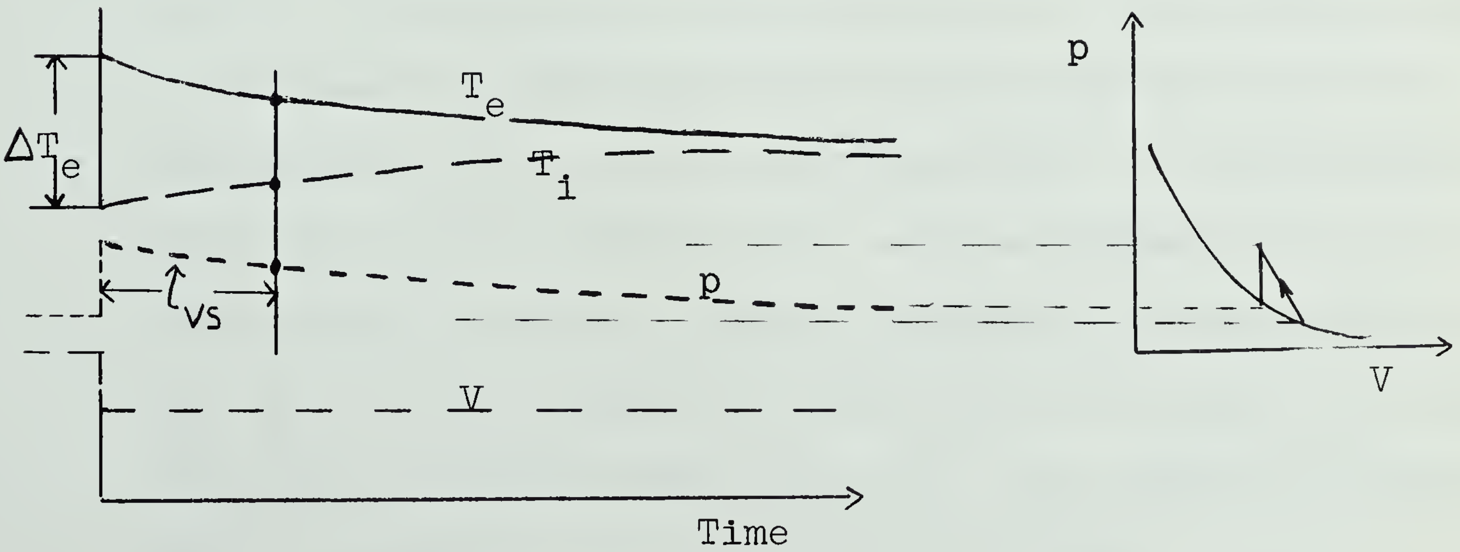
ΔT_e
T_e
T_i
τ_{VS}
p
V
Time
p
V

(c)

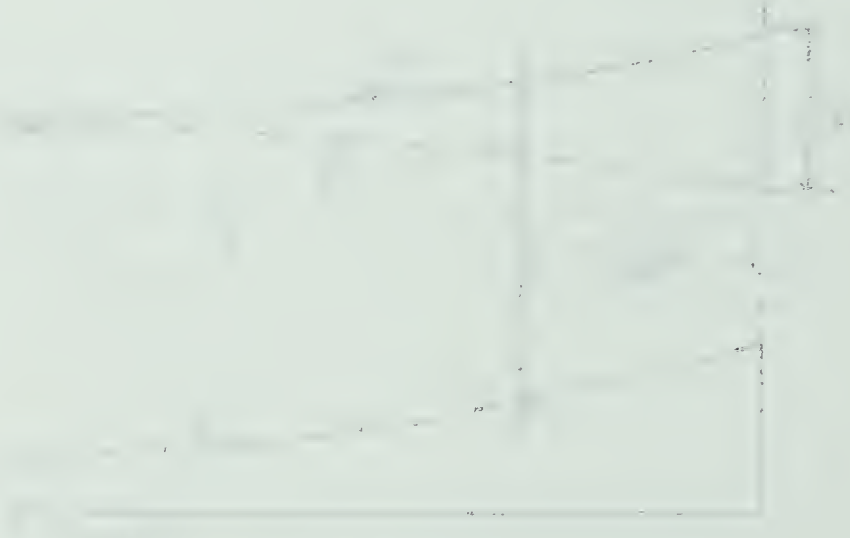

1) depending on the isotopic constitution of the molecules, only two levels are important at temperatures ranging from 20 to 150° K -- when more than two levels are occupied, multiple relaxation processes occur, which are rather difficult to analyse; 2) due to the very small moment of inertia of the hydrogen molecule, the rotational energy levels are widely spaced; 3) the relaxation strength ϵ can be computed easily since physical properties such as the specific heats are well known in the case of hydrogen. These three points will now be examined more closely.

The hydrogen molecule is essentially a rigid rotator whose energy levels are given by the usual formula

$$E_J = J(J + 1)\frac{\hbar^2}{2I}$$

where I is the moment of inertia of the rotator, J is the rotational quantum number, $\hbar$ is Planck's constant divided by 2π. Depending on the orientation of the nuclear spins of the two hydrogen atoms which constitute the molecule, hydrogen can exist in two modifications: orthohydrogen when the total nuclear spin is one, and parahydrogen when the total nuclear spin is zero. Quantum mechanical considerations show that only the odd-numbered rotational states can be occupied in the case of orthohydrogen, and only even-numbered rotational levels can be occupied in the case of parahydrogen.

The thermodynamical equilibrium between the ortho and the para modifications is given by Boltzmann's distribution law, and simple calculations show that at room temperature, orthohydrogen (o-H_2) represents 75% of the equilibrium mixture. At 20°K however, the equilibrium mixture is over 99% parahydrogen (p-H_2). Transitions between the two modifications do not occur except in the presence of a catalyst. For example, in the absence of a catalyst, normal hydrogen (75% ortho - 25% para) does not convert to pure parahydrogen, even when cooled down to 20°K. The relative concentration of ortho and para molecules, 3:1 remains the same. As a result, the ortho and para modifications can be treated as two different gases. In the presence of a catalyst however, almost pure parahydrogen can be obtained by cooling hydrogen down to 20°K.

The occupation of the rotational energy levels as a function of temperature for p-H_2 and o-H_2 appears in figure (3) a) and b) respectively. As can be seen in these figures, below 100°K, parahydrogen is a two-level gas, which can therefore exhibit a single relaxation process, under the influence of a sound wave.

The fact that the hydrogen molecule has a small moment of inertia is of great importance; indeed, the spacing between the rotational energy levels of a molecule is

Fig. 3 a)

Energy level population in parahydrogen.

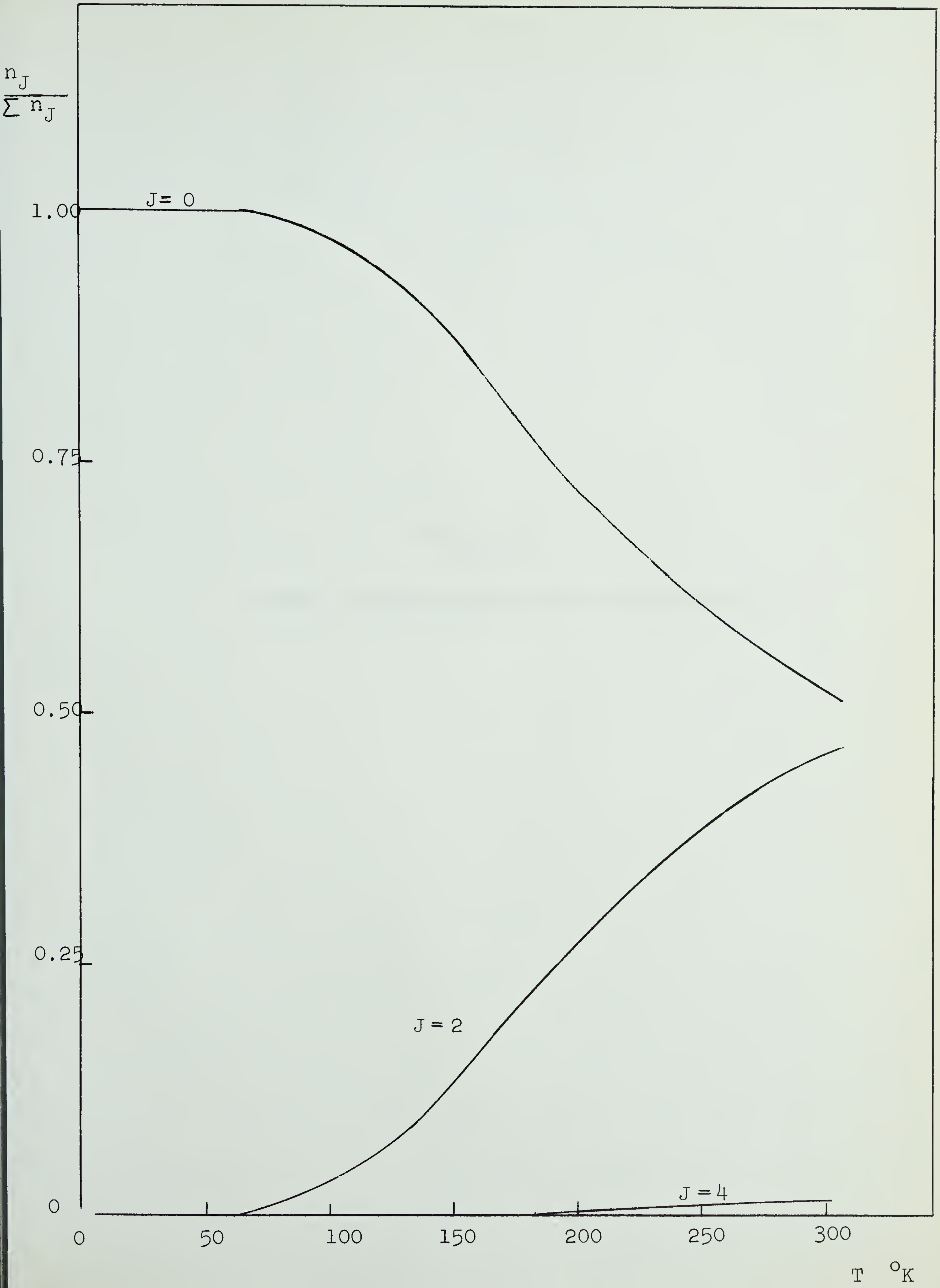
$\frac{n_J}{\sum n_J}$
1.00
0.75
0.50
0.25
0
J= 0
J = 2
J = 4
0
50
100
150
200
250
300
T °K

Fig. 3 b)

Energy level population in orthohydrogen.

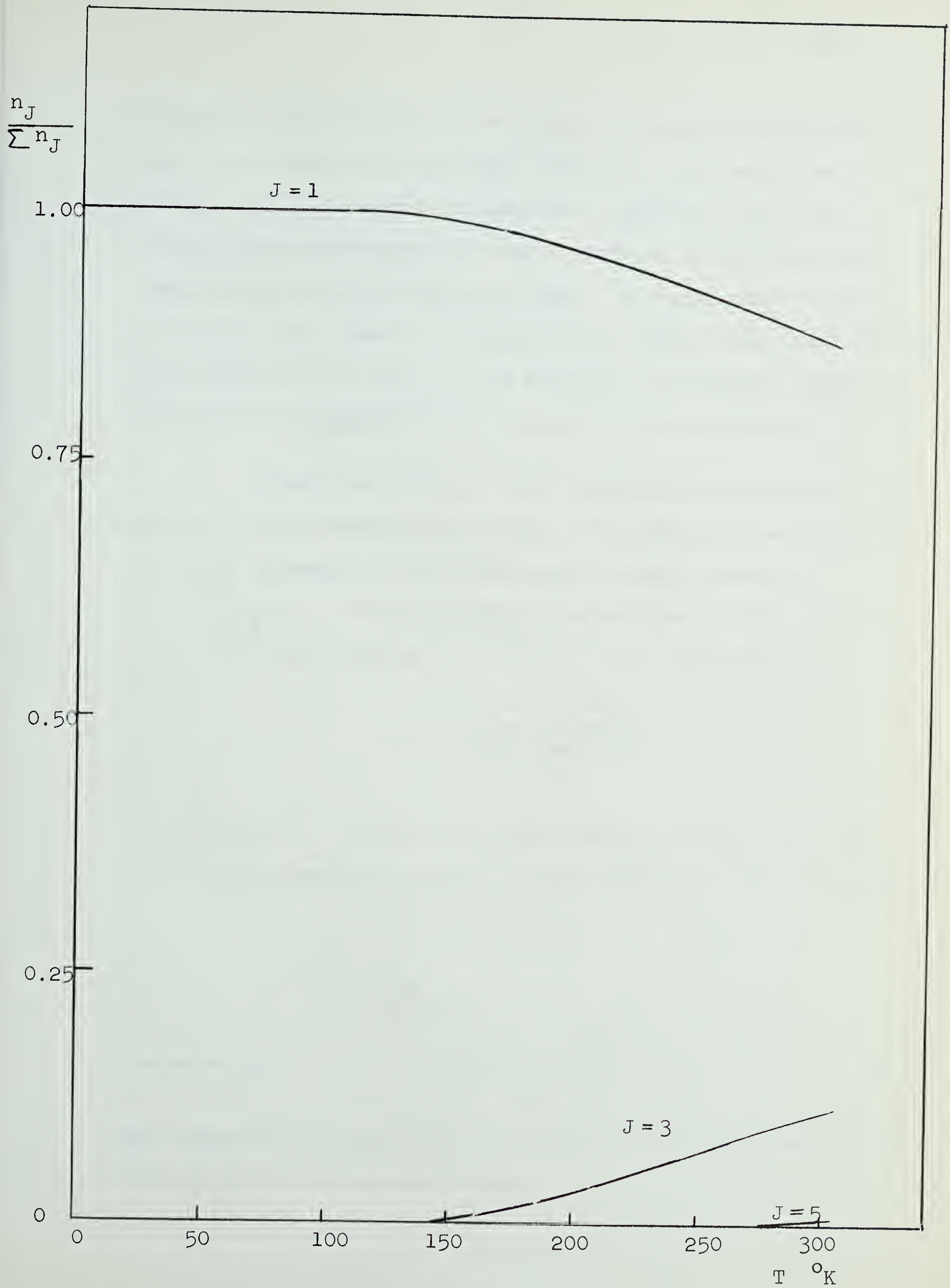
$\frac{n_J}{\sum n_J}$
1.00
0.75
0.50
0.25
0
J = 1
J = 3
J = 5
0
50
100
150
200
250
300
T °K

inversely proportional to the moment of inertia of the molecule, and transitions are less likely to occur when the energy levels are widely separated. Therefore, one can conclude that molecules with small moments of inertia have comparatively long relaxation times. In fact, most molecules have such large moments of inertia that their rotational relaxation times are too short to be measured accurately: hydrogen, deuterium and hydrogen deuteride are a few exceptions.

Equations (1-80), (1-81) and (1-82) contain the factor ϵ, the relaxation strength. As mentioned previously, ϵ is the diameter of the "Cole plot", and is equal to $(1 - \tau_{VS}/\tau_{pS})$. With the help of equations (1-66), (1-67) and (1-68), and putting $K_T^0/K_T^\infty = 1$, one can write

$$\epsilon = \frac{C_V^0 \, C_p^\infty - C_V^\infty \, C_p^0}{C_V^0 \, C_p^\infty}$$

Introducing C' as the rotational specific heat, i.e. that part of the specific heat due to the rotation of the molecule,

$$C_p^\infty = C_p^0 - C'$$

and

$$C_V^\infty = C_V^0 - C' \quad .$$

Consequently, $$\epsilon = \frac{C'(C_p^0 - C_V^0)}{C_V^0 \, (C_p^0 - C')} \quad .$$

The relaxation strength is thus seen to be directly related to the values of the specific heats.

CHAPTER II

EXPERIMENT

1. Experimental Methods

The methods which have been devised for measuring the absorption and the dispersion of sound waves, can be classified into three groups: 1) mechanical, 2) optical, and 3) electrical. In one section of a conprehensive paper on the absorption of sound in fluids, Markham, Beyer and Lindsay[5] made a critical examination of these methods, and the following paragraphs are based on this paper.

Mechanical methods make use of the radiation pressure which is the difference, due to the sound beam, between the pressure on one side of a rigid wall, and the pressure on the other side of the wall, in the medium at rest. The forces being measured are very small, and often of the same order of magnitude as other extraneous forces such as the surface tension. Cavitation effects on the other hand, set an upper limit to the sound intensity. Other factors such as reflections from the walls of the container and divergence of the beam at lower frequencies limit the usefulness and the accuracy of this method. Above 10 Mc/sec, the accuracy is ± 5%, while below 3 Mc/sec, hardly any results obtained by this method, can be relied upon.

Optical methods are based on the fact that when a gas is subjected to a sound wave, the alternating regions of compression and rarefaction act as diffracting elements for a beam of light at right angles to the sound path. The sound beam transforms the gas into a diffraction grating. It is easy to see that such a method imposes stringent experimental requirements: alignment for instance is very critical. Divergence of the sound beam sets a lower limit to the range of frequencies at which experiments can be conducted. Optical methods, like mechanical methods are most trustworthy above 10 Mc/sec.

The majority of measurements on sound absorption and dispersion in gases have been obtained by electrical methods, which include all methods making use of a microphone. Although piezoelectric transducers are the commonest type of microphones, transducers of the condenser type with solid dielectric have proved to be equally reliable and more versatile. Electrical methods can in turn be classified into three groups: a) interferometric, b) direct, and c) pulse.

The first ultrasonic interferometer was built by Pierce in 1925. Shortly after, Hubbard made significant contributions to the field of ultrasonic interferometry. Most of the earlier results on the absorption and dispersion of sound in gases were obtained by this method. An acoustic interferometer is essentially an electromechanical system

composed of a column of fluid set into longitudinal vibrations at one end by an oscillating plate, and terminated at the other end by a reflecting plate. Multiple reflection takes place between the source and the reflector; as the length of the sound path is varied, cyclical changes of phase and amplitude of the forced vibrations occur, the reflector passing through successive positions of resonance in the fluid medium. Due to the nature of the transducer, the variations of pressure at the surface of the vibrator manifest themselves as variations of current, or sometimes of frequency, in the electric circuit coupled to the transducer. Since it is essentially a problem of standing waves, these cyclical changes occur each time the reflector is moved by half a wavelength. The interferometer thus lends itself most conveniently to the measurement of the sound velocity. At first glance, it would appear that the absorption coefficient could be readily obtained from the ratio of the amplitude of two successive maxima. In practise however, many factors such as the reflection coefficient of the reflector have to be taken into account when calculating the absorption coefficient.

Pumper[6] criticized this method and demonstrated that the interferometer can be made to yield differing results by slight modifications of technique. The scatter of the

results obtained by this method for the values of the sound absorption coefficients seem to justify Pumper's criticisms. As stated previously however, the interferometer remains most useful and reliable for measuring the sound dispersion.

In the direct method, a transducer of radius a generates a sound wave of wavelength λ. Within a distance a^2/λ from the emitter, Fresnel diffraction takes place, and the sound beam is cylindrical with a radius a. Within that distance, the amplitude of the sound beam averaged over a cross-section of the cylinder decreases as $e^{-\alpha x}$, where α is the absorption coefficient of the medium, and x is the distance from the source. Standing waves are a problem, although at high enough absorption and at large distances, their effect becomes negligible. Mechanical and electrical cross-talks also give difficulties if they are not neutralized properly. In gases, this method has been applied quite successfully at 3 Mc/sec/atm and higher, in particular, by Meyer and Sessler[7], and by Sluijter, Knaap and Beenakker.[8]

All methods making use of continuous waves present the following disadvantages: standing waves can affect the results, and moreover, if power is continuously dissipated in the form of heat in the medium, the temperature of the fluid may be altered locally, and measurements taken at a temperature higher than that recorded. In the pulse method,

these problems do not arise: if the pulse repetition rate is low enough, standing waves cannot be set up, and if the duty ratio is of the order of 1:500, the heating effect is reduced in the same proportion. The pulse method also permits to distinguish in time, between the received pulse and other unwanted signals. One objection may be raised against the pulse method however; since a short pulse contains a whole spectrum of frequencies, and since the sound absorption varies with the frequency, there is an error involved in taking measurements with short pulses. Pellam and Galt[9] demonstrated that when the absorption coefficient varies as the square of the frequency, and when the pulse contains several oscillations, the error involved is equal to the square of the reciprocal of the number of oscillations per pulse. For example, when a pulse contains ten oscillations, the error is one part in a hundred, which is usually less than the errors associated with the measurement of other parameters, such as the pressure, the voltage etc. The main disadvantage of the pulse method is the poor signal-to-noise ratio associated with the large bandwidth of the receiver.

In conclusion , no method is obviously the best one. A compromise must be reached, which depends on the problem to be solved, as well as on the facilities available in a particular laboratory.

2. Apparatus

In order to observe a single relaxation process in hydrogen, measurements have to be taken at temperatures below 150°K. Since liquid nitrogen was the most readily available refrigerant, a gas vessel was constructed which is suitable for that temperature. Another requirement imposed on the apparatus was the range of frequency-to-pressure ratios (f/p) at which experiments were to be conducted. Since the maximum of the absorption peak for hydrogen occurs at around 10 Mc/sec/atm, the apparatus was built to cover an appropriate range of f/p: from 3 to 50 Mc/sec/atm. Equations (1-80), (1-81) and (1-82) show that τ always appears in the combination $\omega\tau$. Assuming that rotational energy transfer is due to binary collisions only, τ is inversely proportional to the collision rate, and consequently inversely proportional to the pressure. The absorption can thus be measured as a function of f/p, rather than of $\omega\tau$. The proportionality factor between f/p and $\omega\tau$ is independent of frequency and pressure. Since it is easier experimentally to vary the pressure rather than the frequency, measurements were taken at a fixed frequency, for various pressure values.

A. Mechanical part.

A schematic diagram of the cryostat appears in fig. 4. The cryostat is supported vertically and can thus be immersed in a refrigerant bath. The double bellows arrangement, adapted from Stewart,[10] has two advantages: firstly, the volume remains constant while the distance between the two transducers is varied, and secondly, this arrangement constitutes a temperature-resistant motion seal -- other types of motion seals while efficient at room temperature, may not be leak-proof at liquid nitrogen temperature. The elasticity of the bellows permits the length of the sound path to be varied from 1.5 to 14 mm. The position of the movable transducer is determined by means of a micrometer.

Indium O-rings are used as seals between the stainless steel flanges which are soldered to the bellows, and the flanges of the central rigid portion of the cryostat.

Spring loaded adjustment screws permit the transducers to be set as parallel as possible. The right degree of parallelism is achieved when the received signal is maximum. It is also important that this parallelism be maintained as the movable transducer is brought forward or backward: This is the purpose of the driving shaft fixed to the upper plate of the cryostat, which slides inside a tight-fitting bushing.

Fig. 4

Cross Section of Apparatus

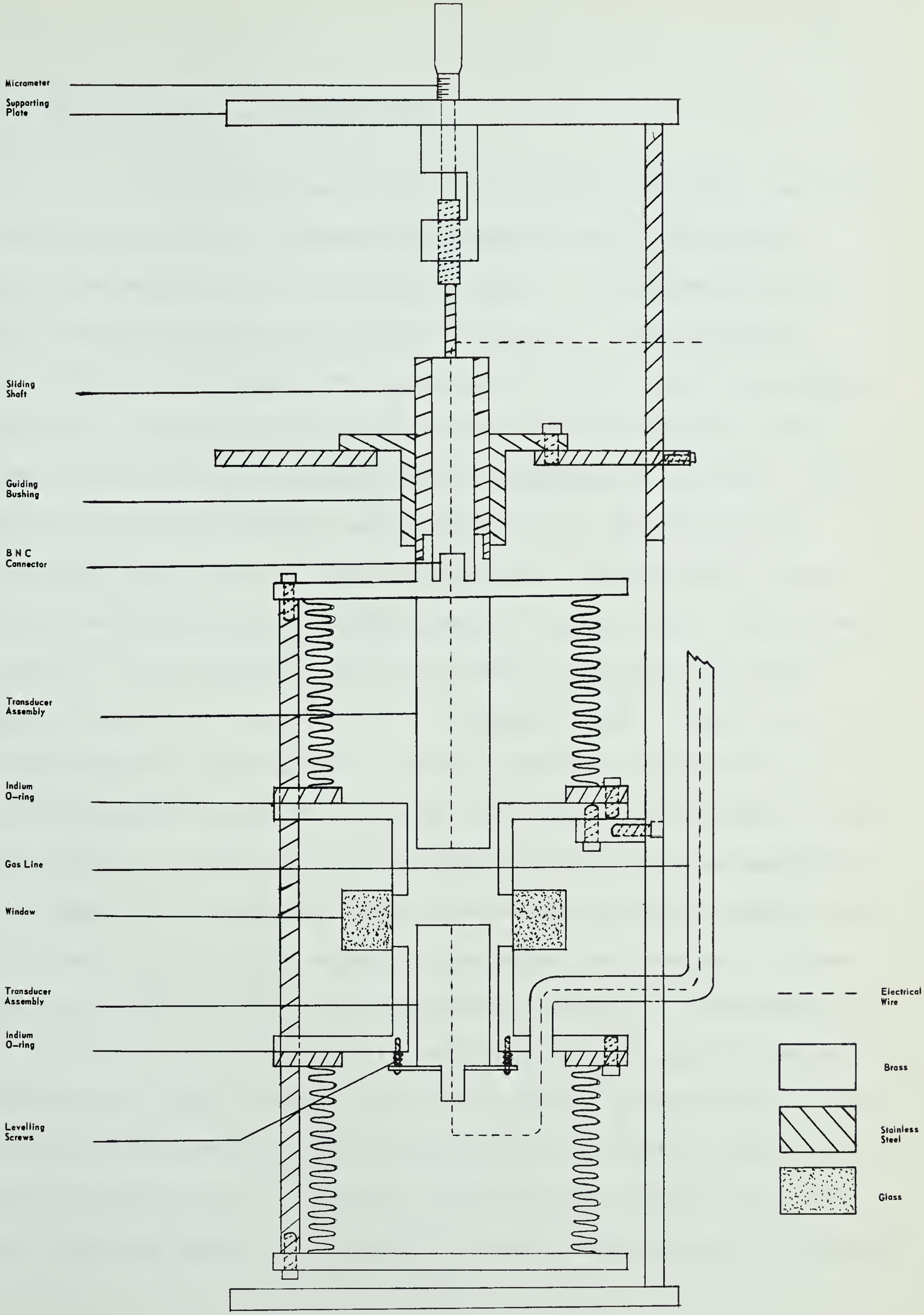
Micrometer
Supporting Plate
Sliding Shaft
Guiding Bushing
B N C Connector
Transducer Assembly
Indium O–ring
Gas Line
Window
Transducer Assembly
Indium O–ring
Levelling Screws
Electrical Wire
Brass
Stainless Steel
Glass

B. Mounting of the Transducers

The transducers are X-cut quartz crystals, one inch in diameter, with a fundamental frequency of 3.00 Mc/sec. They are cemented to a block of Lucite. A cross-section of the transducers support appears in fig. 5. Many attempts were made at providing the transducers with proper electrodes. Films of copper, aluminum and chromium were deposited onto the surfaces of the transducers by evaporation in vacuo. The electrodes thus obtained were too thin and did not adhere satisfactorily to the quartz substrate. Coating the transducers with silver metallizing paint (electrically conducting), proved to be successful to some extent, although the paint had a tendency to dissolve in the grease used to bond the transducers to the Lucite. Another attempt consisted of cementing thin discs of aluminum foil onto the surfaces of the transducers. This also was a rather satisfactory arrangement, although the transducers seemed to be too heavily loaded, with the result that their resonant frequency was lowered. Consequently, the following compromise was reached: the surface of the transducer which is in contact with the gas is coated with silver paint, while the surface which is cemented to the Lucite is covered with an electrode cut out from a sheet of thin aluminum foil. Silicone vacuum grease proved to be the best bonding agent. At liquid nitrogen temperature, the resonant

Fig. 5

Transducers Mount

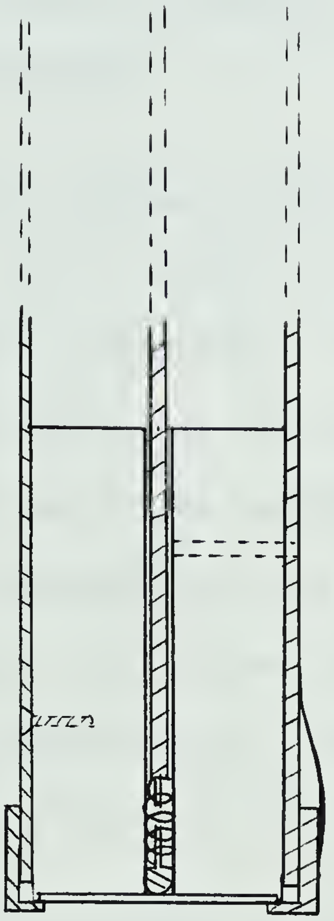

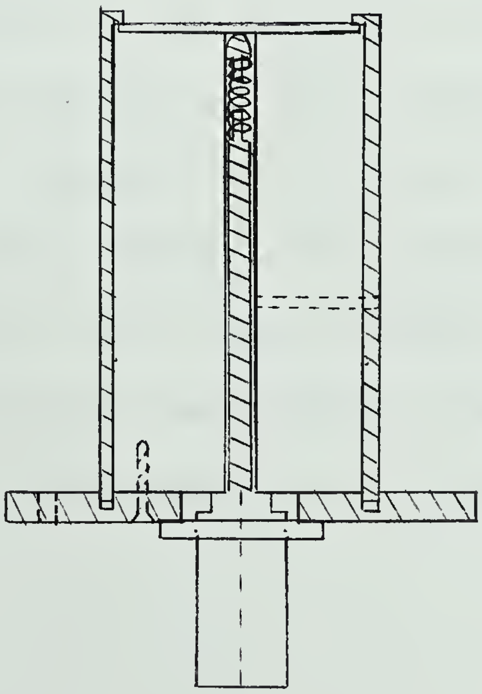

frequency of the transducers is 2.85 Mc/sec. The lowering of the resonant frequency is seemingly due to the extra thickness of the foil and the thin film of grease used to bond the electrode to the quartz crystal.

Unloaded quartz crystals have a very high "Q" factor, which can reach 10,000. Such a highly tuned device cannot respond to a pulse of short duration. In the pulse method, it is thus necessary to reduce the "Q" factor of the transducer, or in other words, to increase its bandwidth. This is achieved by backing the transducer with a high impedance and high loss material. Lucite satisfies these two conditions, and is used to load the transducers. Cemented to a block of Lucite, the quartz crystals have a "Q" of approximately 15.

Electromagnetic shielding of transducers calls for coaxial types of connectors. It is for this reason that the arrangement shown in fig. 5 was adopted: the ground connection is provided by a brass hollow cylinder surrounding the cylindrical block of Lucite through the centre of which passes the "live" connector - a thin brass rod terminated in a spring loaded plug. One end of the brass cylinder is such that it covers the periphery of the transducer's face, thus providing electrical contact to the ground.

C. Vacuum system

The gas vessel is evacuated by means of a mechanical pump capable of an ultimate vacuum of 10^{-3} mm Hg. As a preliminary measure, the apparatus was checked for leaks, and connected to a mercury diffusion pump. After evacuation by means of the diffusion pump, the vessel maintains overnight a vacuum better than 10^{-3} mm Hg.

Pressures are read from a mercury manometer with an accuracy of ± 0.5 mm.

D. Electronic Circuitry

A block diagram of the electronic components appears in fig. 6.

A R.F. pulse of adjustable duration, frequency and repetition rate originates from an oscillator driven by a blocking oscillator. Matching of the transducer to the output of the oscillator is effected by means of a tuned air-core transformer with variable number of turns and variable turns ratio.

The receiving transducer is connected to a preamplifier with tunable input coils. The signal is then amplified in a wide-band amplifier with a maximum gain of 80 db. The video output signal from the amplifier is measured by means of a

Fig. 6

Electronic Circuitry

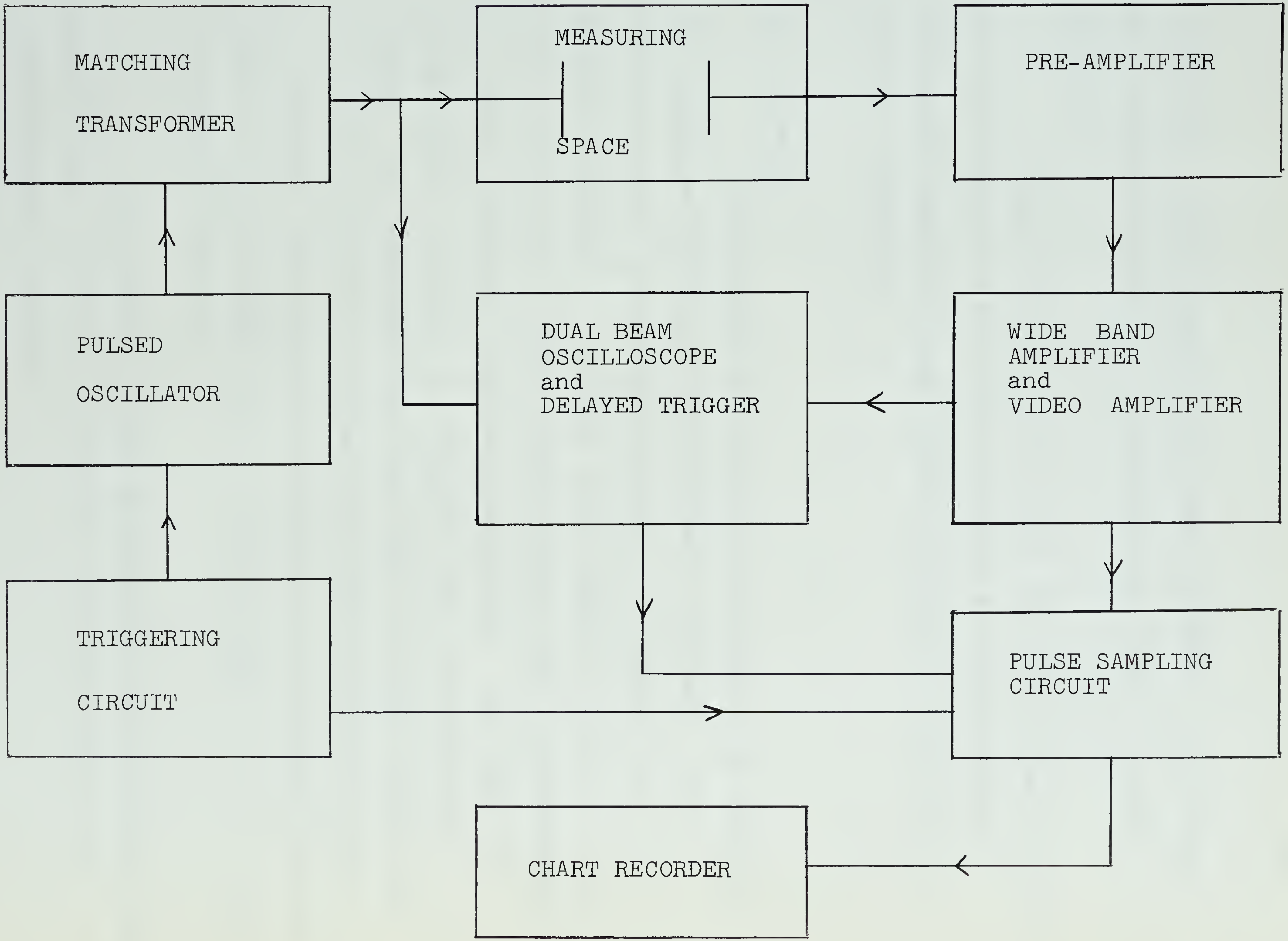
MATCHING
TRANSFORMER
MEASURING
SPACE
PRE-AMPLIFIER
PULSED
OSCILLATOR
DUAL BEAM
OSCILLOSCOPE
and
DELAYED TRIGGER
WIDE BAND
AMPLIFIER
and
VIDEO AMPLIFIER
TRIGGERING
CIRCUIT
PULSE SAMPLING
CIRCUIT
CHART RECORDER

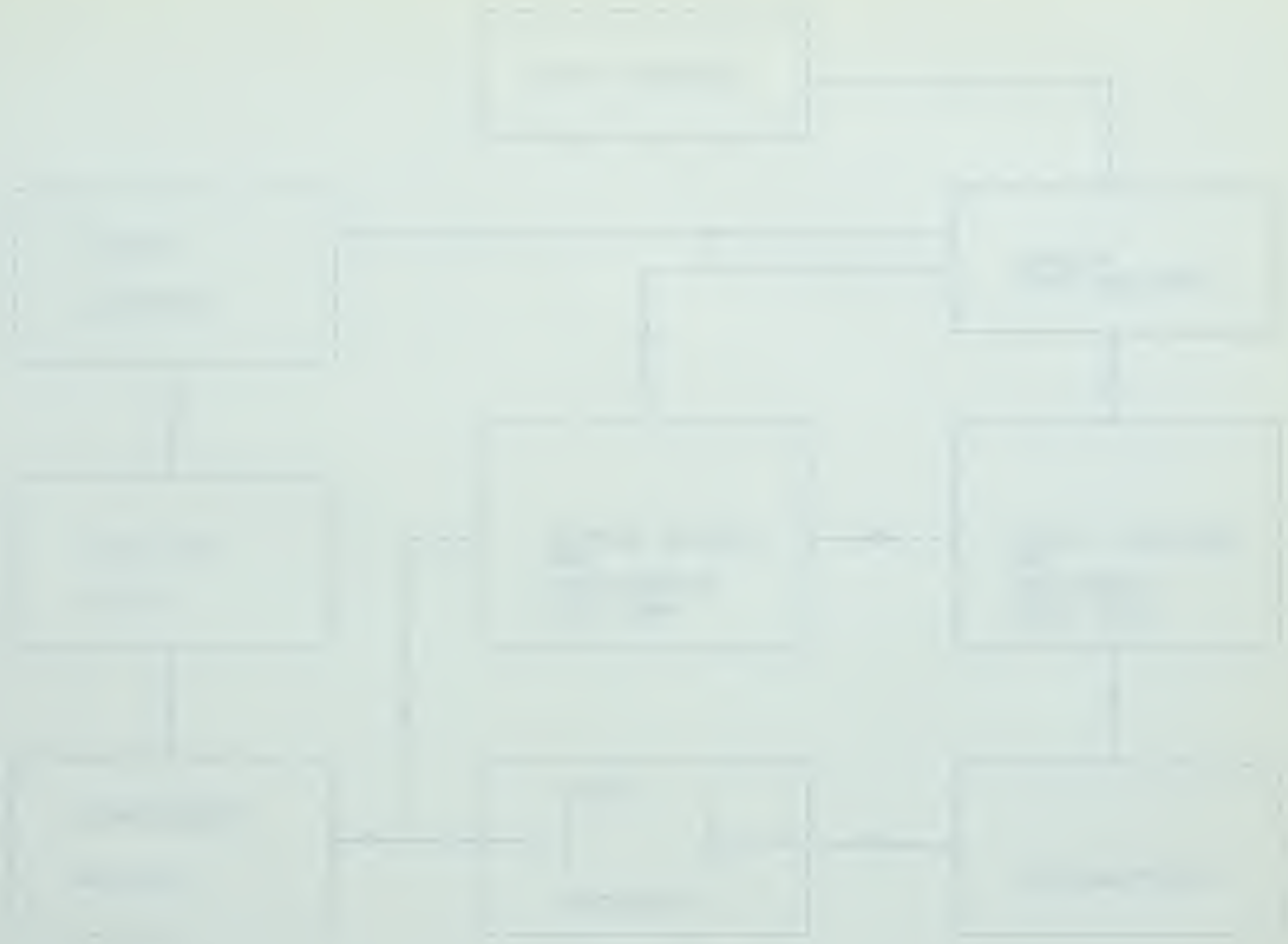

"sampling" circuit adapted from Kamm and Bohm.[11] The output of the sampling circuit is recorded on a 2.5 mv full-scale detector.

Such a method requires that the gain of the amplifier be very stable; for this, all filaments of the amplifying system were heated by large capacity batteries connected to a battery eliminator.

3. Procedure

The cryostat is filled with the gas to be examined, to a pressure slightly above atmospheric pressure. The received signal is recorded at various positions of the movable transducer. A typical record appears in fig. 7. Each record contains in general fifteen double peaks, corresponding to fifteen different transducers separation. The peaks are double since each pulse is "sampled" twice, backward and forward. The amplitudes are then read from these records and the natural logarithm of these amplitudes are plotted versus the distance. The absorption coefficient is determined from the slope of these straight lines. A typical graph of $\ln A$ versus x is shown in fig. 8.

The pressure is then decreased to the next lower value, and the above procedure is repeated, similarly down to the lowest workable pressure.

Fig. 7

Typical Record

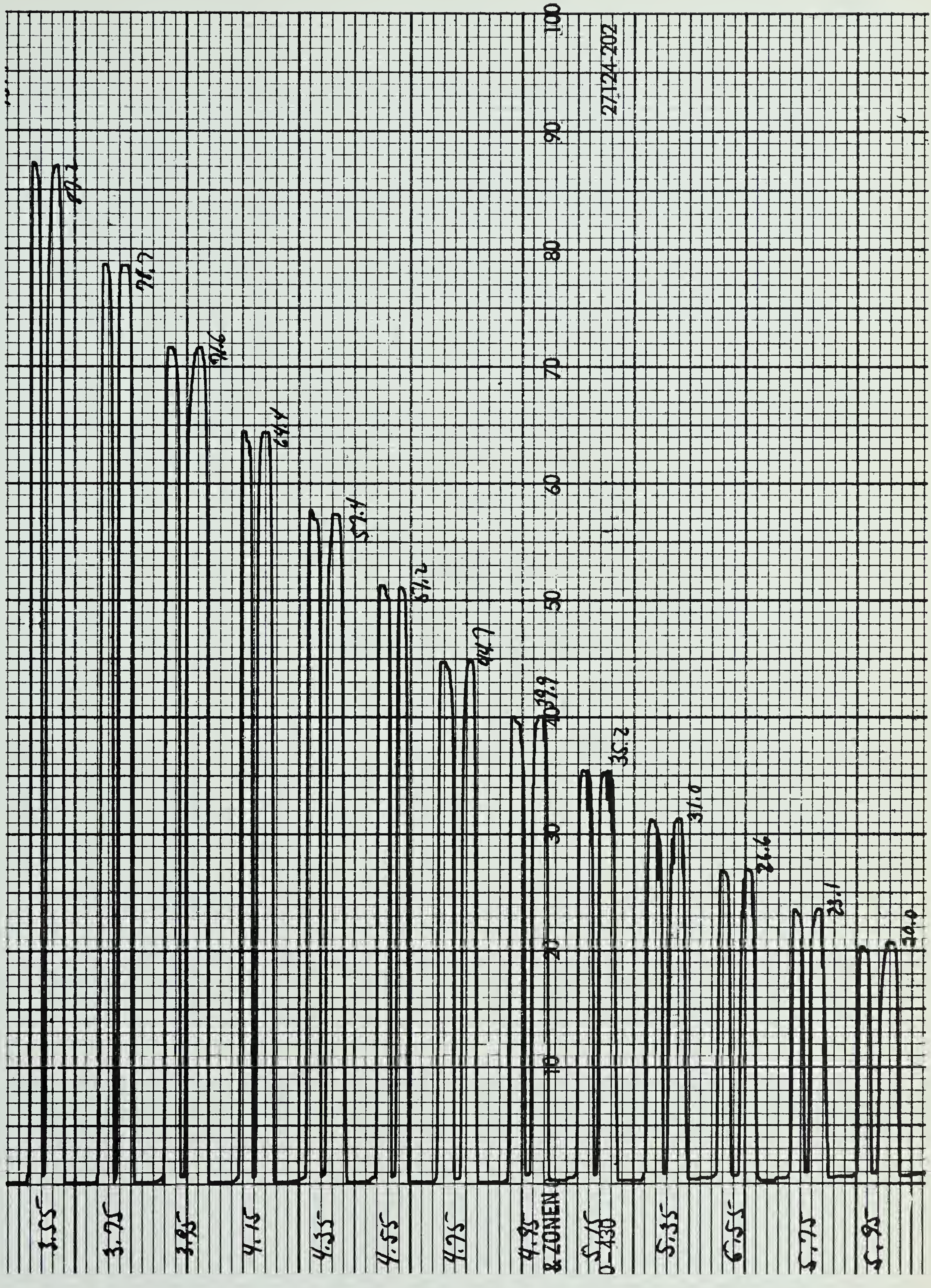
27124-202
100
90
80
70
60
50
40
30
20
10
87.2
78.7
71.6
64.4
57.4
51.2
44.7
39.9
35.2
31.0
26.6
23.1
20.0
3.55
3.75
3.95
4.15
4.35
4.55
4.75
4.95
& ZONEN
5.15
0-430
5.35
5.55
5.75
5.95

Fig. 8

Curve of ln A vs x

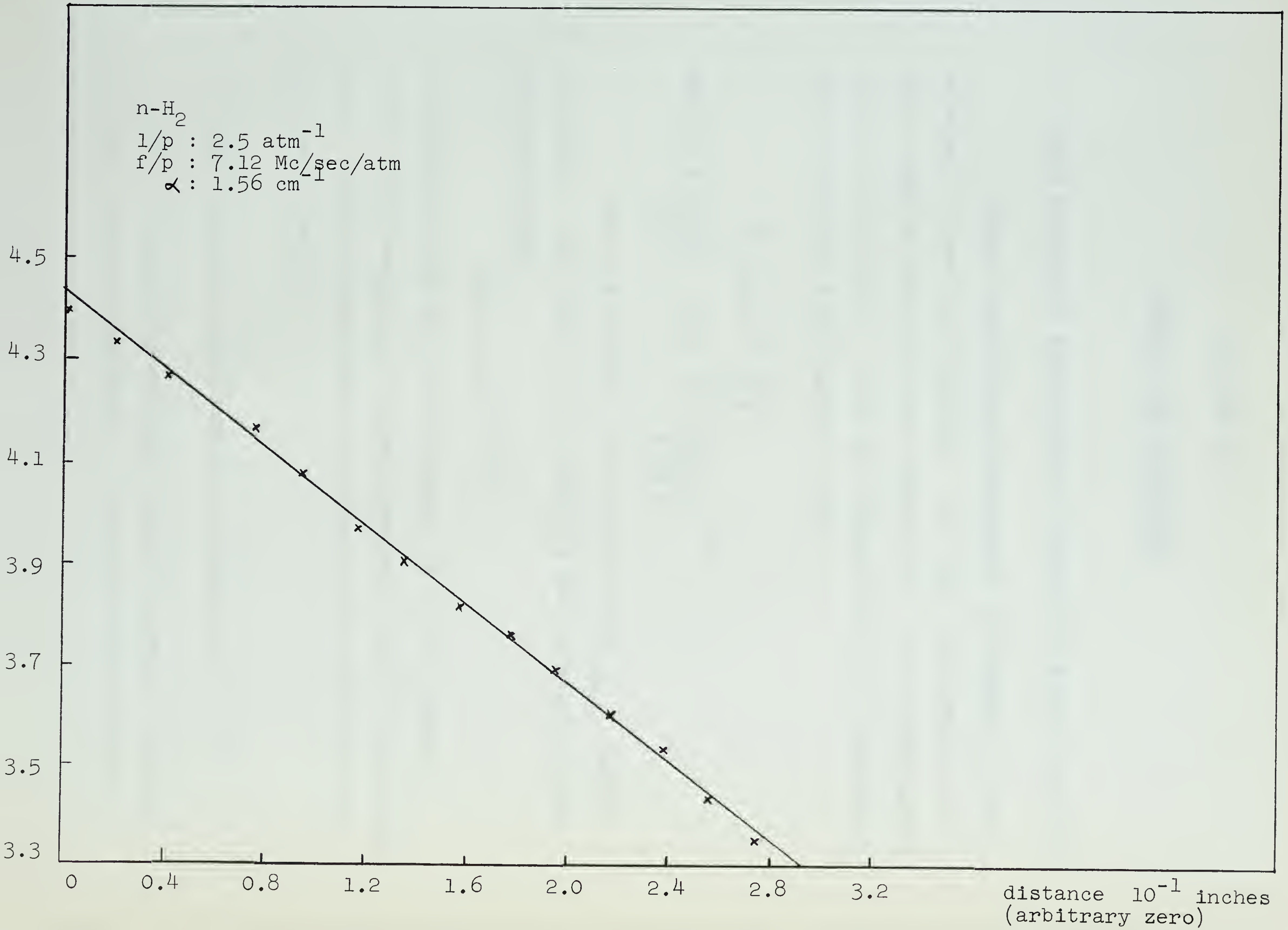
n-H_2
1/p : 2.5 atm^{-1}
f/p : 7.12 Mc/sec/atm
α : 1.56 cm^{-1}
4.5
4.3
4.1
3.9
3.7
3.5
3.3
0
0.4
0.8
1.2
1.6
2.0
2.4
2.8
3.2
distance 10^{-1} inches
(arbitrary zero)

CHAPTER III

RESULTS AND DISCUSSION

1. Sound Absorption Measurements in Helium at Room Temperature

Before undertaking measurements in hydrogen, it was necessary to test the apparatus. For this, measurements were first taken in helium at room temperature. The results appear in fig. 9 and table 2. They are compared with the theoretical curve calculated from equation (1-58)

$$\alpha_{\text{class}} = \frac{7}{6}\frac{1}{R}$$

where $R = \dfrac{\rho_o V_o^2}{\eta\,\omega}$, and $V_o = \left(\dfrac{\gamma p_o}{\rho_o}\right)^{1/2}$.

The data necessary for calculating α_{class} appear in table 1. The value of the viscosity was calculated from Keesom's formula

$$\eta = 5.023\ T^{0.647}$$

in which the units are in micropoises if T is in degrees Kelvin. The results are in good agreement with the theoretical values. The estimated error is certainly less than 10% even at high f/p values.

2. Sound Absorption Measurements in Helium at 76.7 °K.

The apparatus was next tested for proper operation at liquid nitrogen temperature. Due to the low atmospheric

Table 1

Data necessary for the computation of

α class and ϵ.

Table 1

Gas	T	η	φ	C'/R	C_v^o/R	C_p^o/R	γ	V_o	f	$(\alpha p)_{class}$	$\in$
	^oK	μP	10^6 cal $(cm\,^oKsec)^{-1}$					m/sec	Mc/sec	$cm^{-1}atm$	
He	296	119	—	—	1.50	2.50	1.66	995	3.00	0.495	—
He	76.7	82.8	—	—	1.50	2.50	1.66	515	2.85	0.358	—
n-H_2	76.7	34.8	119	0.08	1.58	2.58	1.63	720	2.85	0.103	0.02
p-H_2	76.7	34.8	125	0.29	1.79	2.79	1.55	703	2.85	0.103	0.06

Table 2

Absorption in Helium at 296°K.

Table 2

$1/p$ Atm^{-1}	f/p $\text{Mc}/\text{sec}/\text{atm}$	α cm^{-1}	α/f $(\text{cm Mc}/\text{sec})^{-1}$
1.05	3.15	0.48	0.156
1.34	4.02	0.63	0.210
1.53	4.59	0.805	0.264
1.96	5.88	0.97	0.324
2.57	7.71	1.28	0.430
3.08	9.24	1.52	0.510
3.70	11.1	1.90	0.630
4.10	12.3	2.05	0.680
5.05	15.15	2.40	0.800
5.80	17.4	2.90	0.970
6.20	18.6	3.08	1.03
6.70	20.1	3.50	1.17
7.65	22.95	3.80	1.27
9.20	27.6	4.45	1.48

[illegible]

[illegible]	[illegible]	[illegible]	[illegible]
[illegible]	[illegible]	[illegible]	[illegible]
[illegible]	[illegible]	[illegible]	[illegible]
[illegible]	[illegible]	[illegible]	[illegible]
[illegible]	[illegible]	[illegible]	[illegible]
[illegible]	[illegible]	[illegible]	[illegible]
[illegible]	[illegible]	[illegible]	[illegible]
[illegible]	[illegible]	[illegible]	[illegible]
[illegible]	[illegible]	[illegible]	[illegible]
[illegible]	[illegible]	[illegible]	[illegible]
[illegible]	[illegible]	[illegible]	[illegible]
[illegible]	[illegible]	[illegible]	[illegible]
[illegible]	[illegible]	[illegible]	[illegible]
[illegible]	[illegible]	[illegible]	[illegible]
[illegible]	[illegible]	[illegible]	[illegible]
[illegible]	[illegible]	[illegible]	[illegible]

Figure 9

α/f vs f/p for helium at 296 °K

⊙ Experimental points

- - - - Theoretical curve

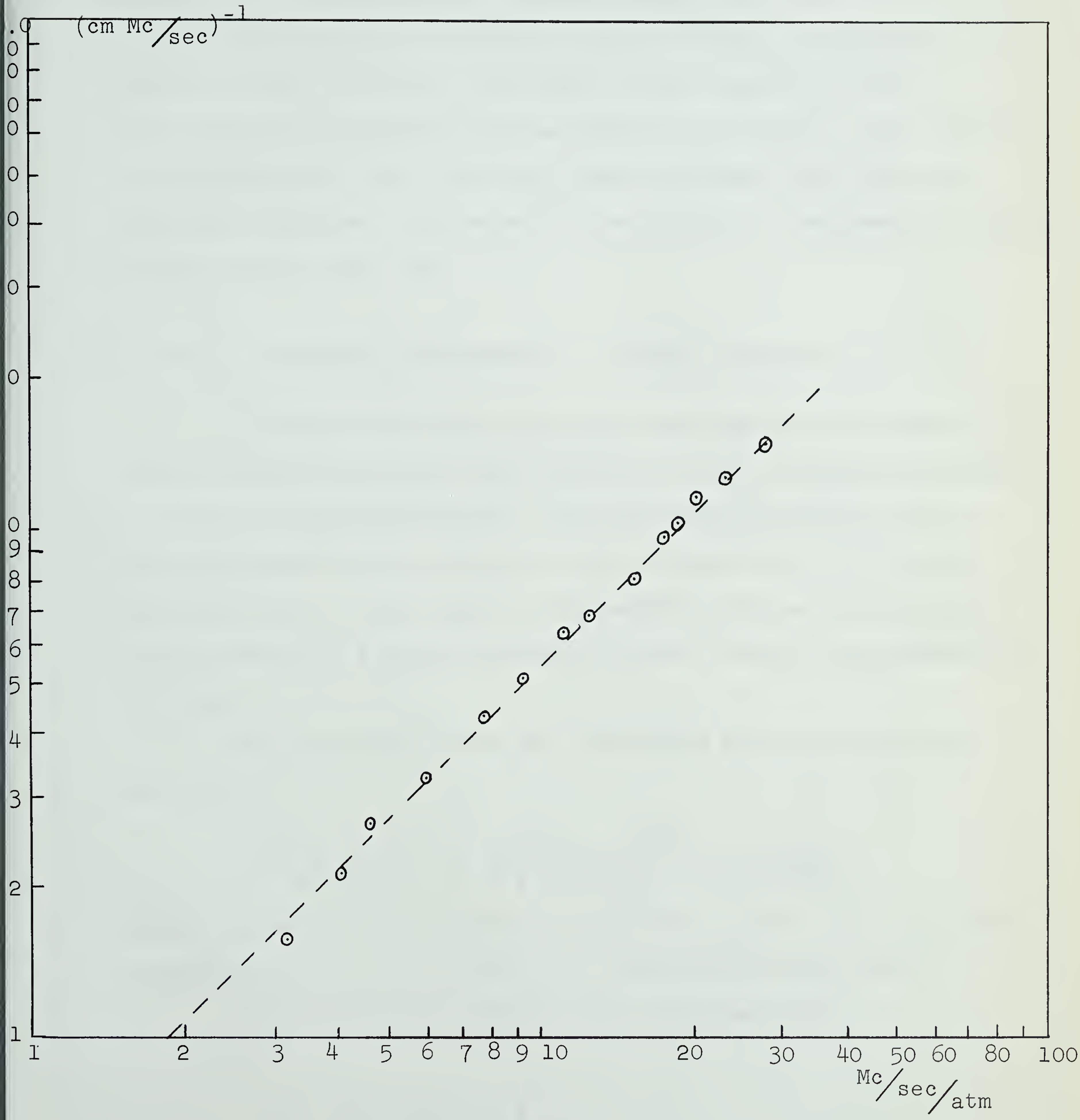

(cm Mc/sec)$^{-1}$
.0
0
0
0
0
0
0
0
0
0
9
8
7
6
5
4
3
2
1
1
2
3
4
5
6
7
8
9
10
20
30
40
50
60
80
100
Mc/sec/atm

pressure in this laboratory, liquid nitrogen boils at 76.7° K.

The results in helium at liquid nitrogen temperature appear in fig. 10 and the individual values figure in table 3. Again, they are compared with the theoretical values. The value of the viscosity was taken this time from Corremans, van Itterbeek, Beenakker, Knaap and Zandbergen[12]. See table 1. The general accuracy is again better than 10%.

3. Sound Absorption Measurements in Normal Hydrogen at 76.7° K.

Although both para and ortho modifications are present in normal hydrogen, the gas should exhibit a single relaxation process at liquid nitrogen temperature, since the first excited level of ortho hydrogen is not populated at that temperature. As can be seen from fig. 11, and table 4, the results obtained in this laboratory indeed fit a single relaxation curve, within the experimental accuracy.

The theoretical curve was calculated from the following expression

$$\alpha'/f = \frac{1}{V_o}\left(1 - \epsilon \frac{\omega^2 \tau^2_{pS}}{1 + \omega^2 \tau^2_{pS}}\right)^{-1/2} \pi \epsilon \frac{\omega \tau_{pS}}{1 + \omega^2 \tau^2_{pS}}$$

which is obtained from equations (1-80) and (1-81). This curve has a maximum at $\tau_{pS} = (1 - \epsilon)^{-1/4}$. (Herzfeld and Litovitz)[13]

The relaxation strength was calculated from

$$\epsilon = \frac{C' \left(C_p^\circ - C_v^\circ\right)}{C_v^\circ \left(C_p^\circ - C'\right)}$$

Table 3

Absorption in helium at 76.7°K.

Table 3

$1/p$	f/p	α	α/f
Atm^{-1}	$\mathrm{Mc}/_{\mathrm{sec}}/_{\mathrm{atm}}$	cm^{-1}	$(\mathrm{cm\ Mc}\ _{\mathrm{sec}})^{-1}$
1.48	4.23	0.52	0.182
2.47	7.02	0.885	0.310
3.30	9.40	1.14	0.400
4.48	12.8	1.80	0.630
5.43	15.4	2.08	0.730
5.80	16.5	2.22	0.778
6.28	17.9	2.52	0.884
6.84	19.6	2.64	0.925
7.23	20.7	2.76	0.968
8.05	22.9	3.07	1.07
8.58	24.4	3.20	1.12
9.30	26.5	3.54	1.24
10.7	30.5	4.13	1.45
12.4	35.4	4.22	1.48
14.8	42.2	5.15	1.81

Figure 10

α/f vs f/p for helium at 76.7° K

⊙ Experimental points

- - - - Theoretical curve

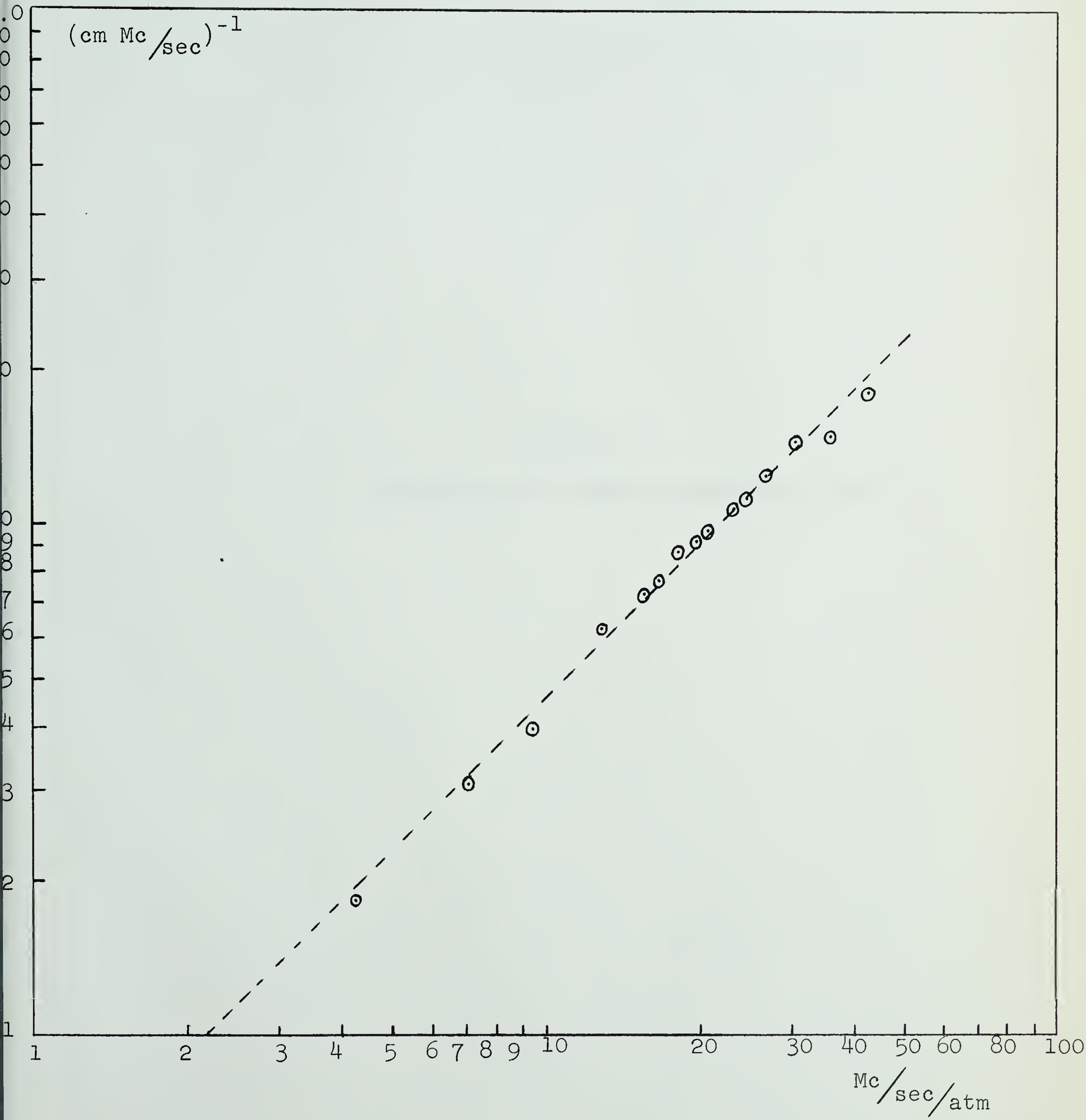
(cm Mc/sec)$^{-1}$
.0
9
8
7
6
5
4
3
2
1
1
2
3
4
5
6
7
8
9
10
20
30
40
50
60
80
100
Mc/sec/atm

Table 4

Absorption in normal hydrogen at 76.7° K

Table 4

f/p $Mc/sec/atm$	α_{class} cm^{-1}	α_{exp} cm^{-1}	α' cm^{-1}	α'/f $(cm\ Mc/sec)^{-1}$
2.42	0.086	0.755	0.67	0.234
3.30	0.118	1.08	0.96	0.330
3.80	0.137	1.09	0.95	0.333
5.02	0.185	1.40	1.22	0.428
5.48	0.194	1.34	1.15	0.403
5.90	0.213	1.46	1.25	0.439
6.62	0.234	1.46	1.23	0.430
7.12	0.258	1.56	1.28	0.450
7.65	0.276	1.61	1.33	0.465
8.15	0.294	1.50	1.21	0.425
8.73	0.316	1.51	1.20	0.421
8.80	0.318	1.60	1.28	0.450
9.60	0.346	1.62	1.27	0.445
10.3	0.372	1.58	1.21	0.423
11.5	0.418	1.63	1.21	0.423
13.0	0.463	1.52	1.06	0.372
16.0	0.570	1.48	0.91	0.318
20.3	0.730	1.54	0.81	0.284
32.3	1.14	1.81	0.67	0.235
45.2	1.60	2.06	0.46	0.160

Figure 11

α'/f vs f/p for normal hydrogen at 76.7° K

⊙ Experimental points

- - - - Theoretical curve calculated for $\epsilon = 0.02$

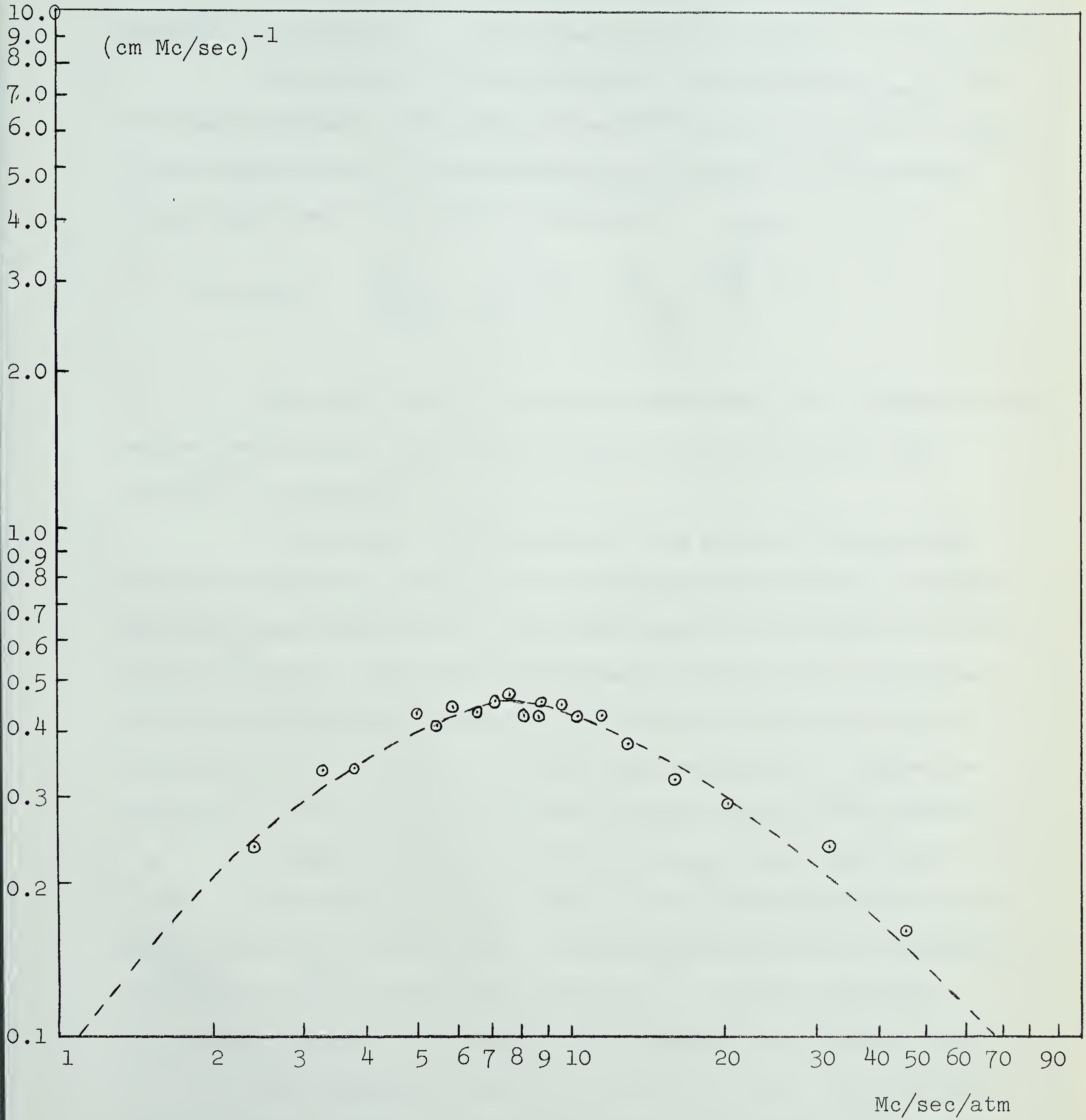

(cm Mc/sec)$^{-1}$
10.0
9.0
8.0
7.0
6.0
5.0
4.0
3.0
2.0
1.0
0.9
0.8
0.7
0.6
0.5
0.4
0.3
0.2
0.1
1
2
3
4
5
6
7
8
9
10
20
30
40
50
60
70
90
Mc/sec/atm

The values of the specific heats were taken from Farkas[14]. See table 1. For normal hydrogen at 76.7° K, $\epsilon = 0.02$.

The value of α' was obtained by subtracting α_{class} from the experimentally determined value of α which is denoted by α_{exp}. Since hydrogen is not a monatomic gas, equation (1-59) rather than (1-58) had to be used in calculating ${}_{class}$:

$$\alpha_{class} = \frac{2\pi^2}{\gamma p_o V_o}\left[\frac{4}{3}\eta + \frac{(\gamma - 1)\phi}{C_p^o}\right] f^2$$

The data for the viscosity were taken from Coremans et al., while the data for the thermal conductivity were taken from Ubbink[15]. See table 1.

In general, the accuracy of the results seems poorer than in the case of helium. It is reasonable however, to assume that α_{exp} was determined to the same degree of accuracy as in the case of helium. The higher discrepancy between the theoretical and the experimental values of α'/f is due to the fact that α' represents only a fraction of the total absorption. Therefore, an error of 10% on α_{exp} constitutes a higher percentage error on α'. For example, at 20.3 Mc/sec-atm , α_{exp} was found equal to 1.54. A 10% error is 0.15. Since α' is obtained by subtracting α_{class} from α_{exp}, α' is 0.81. The absolute error 0.15 represents a relative error of more than 18% on α' . As the classical absorption becomes more important, α' represents a smaller fraction of the total absorption and the accuracy to which α' can be determined becomes lesser. Taking this fact into account, the results

in fig.11 agree with the theoretical curve well within the experimental error.

The maximum of the theoretical curve which best fits the experimental points is located at 7.65 Mc /sec-atm. At this point, $\omega\tau_{pS} = (1 - 0.02)^{-1/4}$. Since τ_{pS} is the adiabatic relaxation time at unit pressure, the maximum of the relaxational absorption occurs at a frequency

$$2\pi \times 7.65 \times 10^{6} \ \mathrm{sec}^{-1}.$$

From this, τ_{pS} is found to be equal to

$$\frac{(1 - 0.02)^{-1/4}}{2\pi \times 7.65 \times 10^{6}} = 2.11 \times 10^{-8} \ \mathrm{sec}.$$

The isothermal or true relaxation time can be calculated from the following relation

$$\frac{\tau_{pS}}{\tau_{pT}} = \frac{C_p^{\infty}}{C_p^{o}} .$$

With $C_p^{o} = 2.58R$ and $C_p^{\infty} = 2.50R$, $\tau_{pT} = 2.17 \times 10^{-8}$ sec.

4. Sound Absorption Measurements in Para-enriched Hydrogen.

An attempt was made at producing pure para hydrogen. Normal hydrogen was liquefied in the presence of a catalyst (hydrous ferric oxide). Since liquid hydrogen is not available in this

laboratory, conversion was effected at a temperature in the neighbourhood of 20° K, above the surface of the liquid inside a ewar containing liquid helium. A few reasons could have contributed to the lack of success of this experiment; the catalyst for instance was probably not activated sufficiently, and the liquified hydrogen may not have been in contact with the catalyst for a long enough time.

Nevertheless, a definite enrichement in para content was achieved, and sound absorption measurements were taken in this para-ortho mixture. The results are shown in fig. 4 and the individual values figure in table 5.

From the maximum value of α'/f, the relaxation strength was found to be equal to 0.045. The theoretical values of the relaxation strength of normal and pure para hydrogen are 0.02 and 0.06 respectively. A relaxation strength of 0.045 corresponds to a rotational specific heat C' of 0.19 R.

The maximum of the absorption curve occurs at a f/p value of 8.1 Mc/sec-atm . From this, τ_{pS} is found to be equal to 1.96×10^{-8} sec. The isothermal relaxation time in this case is

$$\tau_{pT} = 1.96 \times \frac{2.69}{2.50} \times 10^{-8} \text{ sec}$$

or

$$\tau_{pT} = 2.11 \times 10^{-8} \text{ sec},$$

which agrees within a few percent with the isothermal relaxation time for the $0 \longrightarrow 2$ transition found in normal hydrogen.

It is of interest to compare the present results with those obtained by other authors. Sound absorption measurements

Table 5

Absorption in para-enriched hydrogen at 76.7° K

Table 5

f/p Mc sec atm	α_{class} cm^{-1}	α_{exp} cm^{-1}	α' cm^{-1}	α'/f $(cm\ Mc\ sec)^{-1}$
3.03	0.109	1.72	1.61	0.57
4.28	0.154	2.40	2.25	0.79
5.90	0.214	2.68	2.47	0.87
7.10	0.258	2.93	2.67	0.94
8.10	0.293	3.18	2.89	1.01
9.60	0.345	3.08	2.74	0.96
10.6	0.375	3.08	2.71	0.95
11.5	0.415	3.10	2.69	0.92
12.9	0.465	2.83	2.37	0.83
14.6	0.530	2.98	2.45	0.86
16.9	0.610	2.84	2.23	0.78
24.6	0.892	2.67	1.78	0.62
30.9	1.11	2.33	1.22	0.43

Figure 12

α'/f vs f/p for para-enriched hydrogen at 76.7° K

⊙ Experimental points

- - - - Theoretical curve calculated for $\epsilon = 0.045$

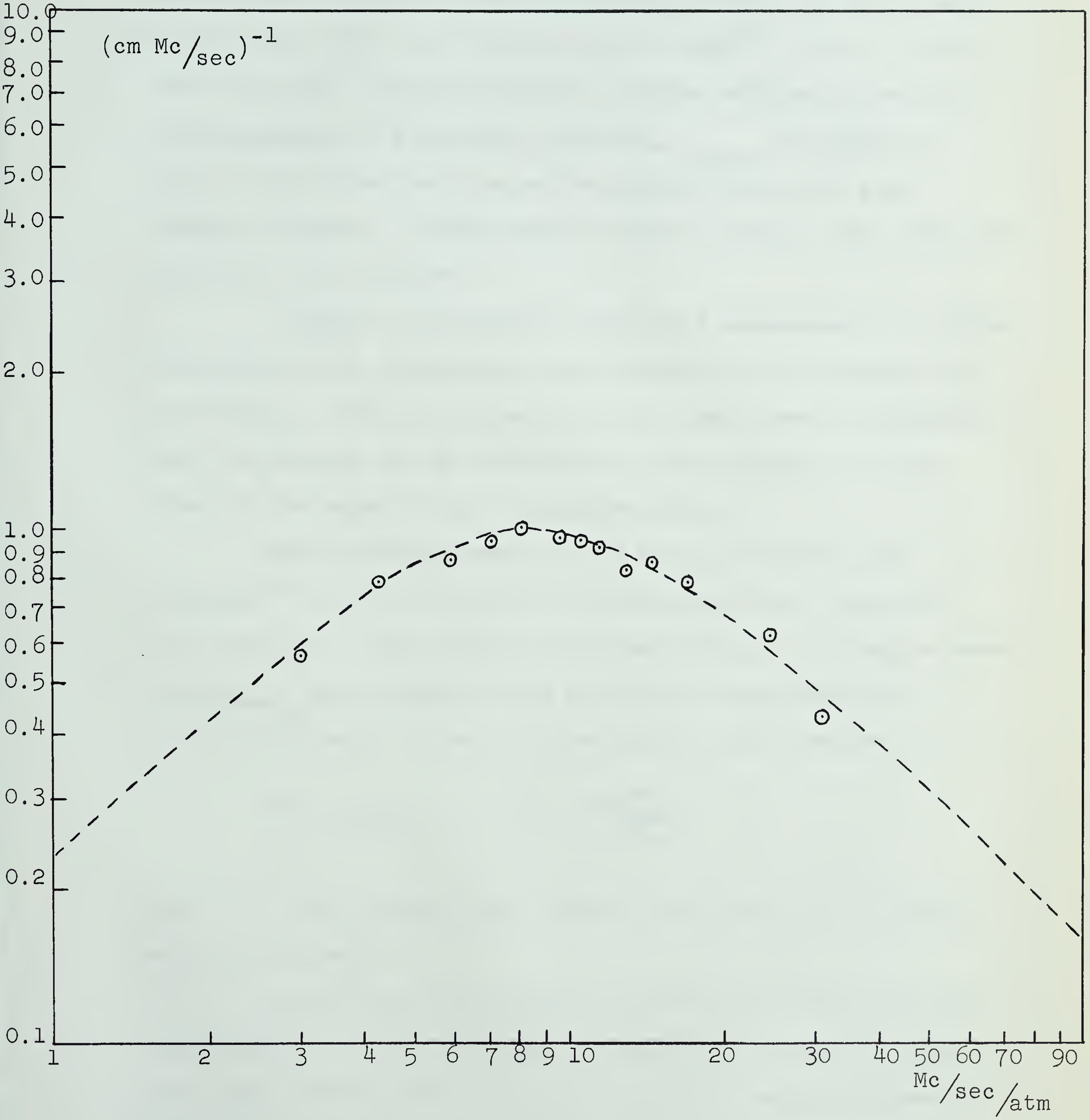
(cm Mc/sec)^-1
10.0
9.0
8.0
7.0
6.0
5.0
4.0
3.0
2.0
1.0
0.9
0.8
0.7
0.6
0.5
0.4
0.3
0.2
0.1
1
2
3
4
5
6
7
8
9
10
20
30
40
50
60
70
90
Mc/sec/atm

in hydrogen have been taken by several authors for many years. In 1937 and 1938, van Itterbeek and Mariens[16], and van Itterbeek and Thys[17] reported results obtained with an ultrasonic interferometer in the region where α/α_{class} is constant, i.e. at f/p values well below the region where α'/f goes through a maximum. These results however did not show the right variation with pressure.

Stewart and Stewart[18] conducted measurements in normal hydrogen with an ultrasonic interferometer at a frequency of 1.95 Mc/sec. With an accuracy of 20%, their results indicated that the maximum of the absorption curve occurred at a f/p value of the order of 10 -- 12 Mc/sec/atm.

Improved measurements taken by van Itterbeek and Verhaegen[19] at 79.5 °K and 90 °K showed the right variation with pressure. These results obtained again in the region where α/α_{class} is constant, yield a value of approximately 2.5×10^{-8} sec. It can be shown that in that region,

$$\alpha/\alpha_{class} = 1 + 0.067 \frac{\tau_{pT}}{\tau_c}$$

where τ_c is the average time between collisions at a pressure of one atmosphere.

Using the pulse method, Parbrook and Tempest[20] took measurements in normal hydrogem at 298 °K. The results show a lower and broader curve which does not fit a single-relaxation curve. This is to be expected since at room temperature, normal hydrogen has five excited levels giving rise to four

possible transitions, with possibly four different relaxation times.

All measurements made in either pure para hydrogen or in normal hydrogen above 150 °K have to be interpreted in terms of two or more relaxation processes. This necessitates the use of many assumptions. In order to analyse the results which he obtained at 293 °K in normal hydrogen, Sessler[21] made the following assumptions: the relaxation time for the $1 \longrightarrow 3$ transition is 1.5 times that for the $0 \longrightarrow 2$ transition, and the relaxation time for the $3 \longrightarrow 5$ transition is the same as that for the $1 \longrightarrow 3$ transition. He assumed moreover that all transitions occur independently. From this, Sessler found that at room temperature the isothermal relaxation time for the $0 \longrightarrow 2$ transition (τ_{02}) is 1.29×10^{-8} sec.

Geide[22] who took measurements in pure para hydrogen at 293 °K, also assumed that the $2 \longrightarrow 4$ transition occurs independently of the $0 \longrightarrow 2$ transition. With this assumption, his measurements yield a value of $\tau_{02} = 1.21 \times 10^{-8}$ sec.

It must be emphasized that these relaxation times (1.29 and 1.21×10^{-8} sec) were obtained from measurements taken at room temperature, and it is reasonable to expect that they should differ from the relaxation times obtained from measurements taken at lower temperatures.

The following considerations will give an idea of the way in which the relaxation times can be expected to vary with temperature.

As was pointed out at the end of the first chapter, the isothermal relaxation time at unit concentration is the reciprocal of the sum of the reaction rates. In para hydrogen

$$\tau_T^{-1} = R_{02} + R_{20} \quad .$$

The relation between R_{02} and R_{20} is provided by the condition of statistical equilibrium,

$$R_{20} = R_{02} \left(\frac{g_o}{g_2} \right) e^{E/kT}$$

where g_o and g_2 are the statistical weights of the rotational levels $J=0$ and $J=2$ respectively. E is the energy difference between the energy of the state $J=2$ and $J=0$.

Now, the reaction rate is proportional to the number of molecules striking unit area per unit time at pressure p and temperature T. From kinetic theory, this number of molecules is $\left(\frac{8}{\pi mkT} \right)^{1/2} p$. The reaction rate is also proportional to the efficiency of the collisions in inducing rotational energy transfer. The efficiency of the collisions is expressed in terms of an averaged inelastic cross section for the $0 \longrightarrow 2$ transition at temperature T and pressure p. This cross section is denoted by $\langle Q_{02} \rangle_T$. Therefore,

$$R_{02} = \left(\frac{8}{\pi mkT} \right)^{1/2} p \langle Q_{02} \rangle_T \quad ,$$

and

$$\tau_T^{-1} = \left(\frac{8}{\pi mkT}\right)^{1/2} p \langle Q_{02} \rangle_T \left(1 + \frac{g_o}{g_2} e^{E/kT}\right) .$$

$\langle Q_{02} \rangle_T$ is obtained gy averaging Q(K), the inelastic cross section corresponding to a wave number K, over the Maxwellian distribution of wave numbers K at temperature T.

Various authors[25, 26, 27] have calculated Q(K) for different forms of the intermolecular potential. Using a Morse-type potential with two angle-dependent terms, Davison[25] has computed the values of Q(K) as function of K^2. His results may be approximated as follows:

$$Q(K) = c\ (K^2 - K_o^2)$$

where c = 0.043 and $K_o^2 = 6$ in atomic units. In this system of units, Planck's constant is equal to 2π.

Averaged over the Maxwellian distribution of wave numbers at temperature T, Q(K) yields

$$\langle Q_{02} \rangle_T = \exp\ (-E/kT)\ 4cmkT \left(1 + E/2kT\right) .$$

Inserting $\langle Q_{02} \rangle_T$ into the expression for τ_T^{-1}, one gets

$$\tau_T^{-1} = \left(\frac{8}{\pi mkT}\right)^{1/2} p \left[\frac{g_o}{g_2} + \exp\ (-E/kT)\right] 4cmkT \left(1 + E/2kT\right) .$$

Above 150 °K, the factor $T^{-1/2}$ is dominant and one should expect the relaxation times to decrease as the temperature

increases.

A rough calculation shows that the relaxation time at room temperature should be approximately half the relaxation time at liquid nitrogen temperature.

Indeed,

at 80 °K, $E/kT \approx 1$ and $e^{-1} \approx 0.37$;

at 300 °K, $E/kT \approx 0.3$ and $e^{-0.3} \approx 0.72$;

$g_0 = 1$ and $g_2 = 3$.

Therefore,

$$\frac{\tau_{300}}{\tau_{80}} \approx \left(\frac{80}{300}\right)^{1/2} \times \frac{(0.33 + 0.37)}{(0.33 + 0.72)} \times \frac{(1 + 0.5)}{(1 + 0.15)}$$

$$\frac{\tau_{300}}{\tau_{80}} \approx 1/2 .$$

The relaxation time deduced from Sessler's measurements at room temperature (1.2×10^{-8} sec) is roughly half the relaxation time deduced from measurements at liquid nitrogen temperature (2.1×10^{-8} sec).

The computation of $\langle Q_{02} \rangle_T$ involves many assumptions and especially, the use of certain adjustable parameters. One may question the validity of the assumptions made, as well as the values of the parameters used. The best way of verifying the reliability of the theory consists of comparing the theoretical and the experimental results over a wide range of temperature. In that respect, τ_T is not the best quantity to consider for making comparisons, because the temperature dependence of

τ_T is affected by the fact that τ_T depends on the number of molecules hitting unit area per unit time. As seen previously, the relaxation time is inversely proportional to the number of molecules hitting unit area per unit time; it is thus proportional to the mean time between collisions τ_c . At pressure p,

$$\tau_c^{-1} = \pi\sigma^2 \left(\frac{8}{\pi mkT}\right)^{1/2} p$$

where σ is the diameter of the molecules treated as hard spheres.

Consequently, the collision number $Z = \tau_T/\tau_c$ is better suited for comparisons between theory and experiment. Using the expressions for τ_T^{-1} and τ_c^{-1} ,

$$Z^{-1} = \frac{\langle Q_{02}\rangle_T}{\pi\sigma^2} \left(1 + \frac{g_o}{g_2} e^{E/kT}\right) .$$

Since $\langle Q_{02}\rangle_T$ results from averaging Q(K) over the Maxwellian distribution of the wave numbers at temperature T, it can be written as

$$\langle Q_{02}\rangle_T = \exp(-E/kT)\, I(T)$$

where I(T) stands for an integral which depends on the form of the intermolecular potential. With $\langle Q_{02}\rangle_T$ expressed as above,

$$Z^{-1} = \frac{1}{\pi\sigma^2}\left[\frac{g_o}{g_2} + \exp(-E/kT)\right] I(T) .$$

Therefore, the temperature dependence of Z is seen to be mostly determined by the temperature dependence of I(T).

Taking $I(T) = 4cmkT\left(1 + E/2kT\right)$ as before,

$$\frac{Z_{300}^{-1}}{Z_{80}^{-1}} \approx \frac{(0.33 + 0.72)}{(0.33 + 0.37)} \times \frac{(1 + 0.15)}{(1 + 0.5\ )} \times \frac{300}{80}$$

$$\frac{Z_{80}}{Z_{300}} \approx 4 \ .$$

This value is in good agreement with the experimental results:

at 300 °K, $\tau_c = 0.7 \times 10^{-10}$ sec,

at 80 °K, $\tau_c = 0.3 \times 10^{-10}$ sec.

Consequently, using Sessler's value of the relaxation time at room temperature,

$$Z_{300} \approx \frac{1.2 \times 10^{-8}}{0.7 \times 10^{-10}} \approx 170 \text{ collisions.}$$

At liquid nitrogen temperature,

$$Z_{80} \approx \frac{2.1 \times 10^{-8}}{0.3 \times 10^{-10}} \approx 700 \text{ collisions.}$$

These values of the collision numbers are in good agreement within an order of magnitude, with the theoretical values deduced from the calculations of Sluijter et al.[24], and those of Brout[30].

The only results obtained in hydrogen below 150 °K, which are reported in the literature, are those of Sluijter, Knaap and Beenakker[8, 23,24]. From their measurements taken in

[illegible]

$$[illegible]$$

[illegible]

[illegible]

$$[illegible]$$

[illegible]

$$[illegible]$$

[illegible]

$$[illegible]$$

[illegible]

[illegible]

pure para hydrogen at 77.3 °K and 90 °K, the values of τ_{02} are found to be 2.2 X 10^{-8} sec and 2.1 X 10^{-8} sec respectively.

Measurements by Sluijter et al. in normal hydrogen at 77.3 °K, however indicated that the maximum of the relaxational absorption occurred at approximately 11 Mc/sec/atm or even higher. This indicated a value of $\tau_{02} = 1.4 \times 10^{-8}$ sec.

This important difference between the relaxation time of para hydrogen at 100% concentration, and the relaxation time at 25% concentration (2.2 X 10^{-8} sec and 1.4 X 10^{-8} sec respectively), raises the question as to whether τ_{02} is the same when collisions occur between para molecules only, as it is when para and ortho molecules collide together. A shorter relaxation time in the case of normal hydrogen would mean that ortho molecules are more efficient than para molecules at inducing rotational energy transfer during a collision.

The present results seem to indicate that such is not the case, since the values of τ_{02} obtained from measurements in normal hydrogen are in good agreement with the value of τ_{02} obtained by Sluijter et al. from measurements in pure para hydrogen.

CONCLUSION

By means of the pulse technique at liquid nitrogen temperature, the sound absorption was measured in normal and para-enriched hydrogen at frequency-to-pressure ratios in the range 3 to 50 Mc/sec/atm.

These measurements are in good agreement with the theory first proposed by Herzfeld and Rice, both as to their dependence on f/p and their absolute magnitude.

The peak in the absorption curve, referred to a pressure of one atmosphere, occurs when $\omega^{-1} = \tau_{pS}$, the adiabatic relaxation time. From this, $\tau_T = \tau_{02}$ was deduced, and the value obtained was $\tau_{02} = 2.1 \times 10^{-8}$ sec, for both para-enriched and normal hydrogen.

This value of τ_{02} is in good agreement with that deduced from measurements taken by the direct method at the same temperature, in pure para hydrogen. It differs however from the value of τ_{02} deduced from measurements taken by other authors in normal hydrogen at the same temperature.

Although no claim is made at a particularly high experimental accuracy, the fact that the number of measurements (i.e. the number of points on the absorption curve) taken in normal hydrogen at liquid nitrogen temperature and reported in this thesis, is considerably larger than the number of similar measurements taken and reported by any other authors, may confer to the present results a certain degree of reliability.

The relaxation theory of Herzfeld and Rice is a thermodynamical one and as such can only provide a macroscopic description of the phenomenon involved. A comparison of the relaxation times obtained at liquid nitrogen temperature, with those obtained by other authors at room temperature shows that the microscopic theory predicts quite satisfactorily the temperature variation of the relaxation times. A full verification of the microscopic theory must however await experimental results at other temperatures. Moreover, theories are not precise enough at the present time to give absolute magnitude of the relaxation times to better than within an order of magnitude.

As yet, no reliable information has been obtained about the relaxation time of the $1 \longrightarrow 3$ transition in ortho hydrogen. If measurements could be performed in pure ortho hydrogen, the results would be most interesting. Unfortunately, the production of ortho hydrogen although feasable[29], remains difficult especially in view of the large amount of gas necessary to fill a cryostat. Measurements in normal hydrogen or in various mixtures of ortho and para hydrogen between 140 °K and 180 °K could also provide some information about the relaxation time of the ortho modification. Results in ortho hydrogen would constitute another way of verifying the microscopic theories.

BIBLIOGRAPHY

1. H. J. Bauer, Physical Acoustics (W.P. Mason), 2, part A, p. 47 (1965).
2. S. R. de Groot and P. Mazur, Non-Equilibrium Thermodynamics North-Holland Publishing Co. Amsterdam, p. 315 (1961)
3. M. Greenspan, J. Acoust. Soc. Am., 22, p. 568 (1950).
4. H. O. Kneser, Physical Acoustics (W. P. Mason), 2, part A p. 133 (1965); Ann. d. Phys., 16, p. 360, (1933).
5. J. J. Markham, R. T. Beyer and R. B. Lindsay, Rev. Mod. Phys., 23, p. 353 (1951).
6. E. J. Pumper, J. Phys. USSR, 1, p. 411 (1939).
7. E. Meyer and G. Sessler, Z. Physik, 149, p. 15 (1957).
8. C. G. Sluijter, H. F. P. Knaap and J. J. M. Beenakker, Physica, 30, p. 745 (1964).
9. J. R. Pellam and J. K. Galt, J. Chem. Phys., 14, p. 608, (1946).
10. J. L. Stewart, Rev. Sci. Instr., 17, p. 59 (1946).
11. G. N. Kamm and H.V. Bohm, Rev. Sci. Instr., 33, p. 957 (1962).
12. J. M. J. Coremans, A. van Itterbeek, J. J. M. Beenakker, H. F. P. Knaap and P.Z. Zandbergen, Physica 24, pp 557 and 1102 (1958).
13. K. F. Herzfeld and A. L. Litovitz, Absorption and dispersion of ultrasonic waves, Academic Press, N. Y. and London (1959).
14. A. Farkas, Orthohydrogen, parahydrogen and heavy hydrogen University Press, Cambridge, (1935).
15. J. B. Ubbink, Physica, 14, p. 165 (1948).
16. A. van Itterbeek and P. Mariens, Physica, 4, p. 609 (1937).
17. A. van Itterbeek and L. Thys, Physica, 5, p. 889 (1938).
18. E. S. Stewart and J. L. Stewart, J. Acoust. Soc. Am., 24, p. 194 (1952).

19. A. van Itterbeek and L. Verhaegen, Nature, 167, p. 478 (1951).

20. H. D. Parbrook and W. J. Tempest, J. Acoust. Soc. Am., 30, p. 985 (1958).

21. G. Sessler, Acustica, 10, p. 176 (1960).

22. K. Geide, Acustica, 13, p. 31 (1963).

23. C. G. Sluijter and R. M. Jonkman, Physica 30, p. 1670 (1964).

24. C. G. Sluijter, H. F. P. Knaap and J. J. M. Beenakker, Physica, 31, p. 915 (1965).

25. W. D. Davison, Disc. Far. Soc., 33, p. 71 (1962).

26. C. S. Roberts, Phys Rev., 131, p. 209 (1963).

27. K. Takayanagi, Suppl. Prog. Theor. Phys., 25, p. 1 (1963).

28. K. F. Herzfeld and F. O. Rice, Phys. Rev., 31, p. 691 (1928).

29. L. Bachmann, E. Bechtold and E. Cremer, J. Catalysis, 1, p. 113 (1962).

30. R. Brout, J. Chem. Phys., 22, p. 934 (1954).

B29860